AUS DER FAKULTÄT FÜR BIOLOGIE UND VORKLINISCHE MEDIZIN
DER UNIVERSITÄT REGENSBURG
PROF. DR. GERNOT LÄNGST

CHARACTERIZATION OF STABLE CELL LINES, INDUCIBLY CO-EXPRESSING CHD3/4 WITH PU.1

Inaugural – Dissertation
zur Erlangung des Doktorgrades
der Medizin

der
Fakultät für Medizin
der Universität Regensburg

vorgelegt von
Michael F. Siegel

2022

AUS DER FAKULTÄT FÜR BIOLOGIE UND VORKLINISCHE MEDIZIN
DER UNIVERSITÄT REGENSBURG
PROF. DR. GERNOT LÄNGST

CHARACTERIZATION OF STABLE CELL LINES, INDUCIBLY CO-EXPRESSING CHD3/4 WITH PU.1

Inaugural – Dissertation
zur Erlangung des Doktorgrades
der Medizin

der
Fakultät für Medizin
der Universität Regensburg

vorgelegt von
Michael F. Siegel

2022

Dekan: Prof. Dr. Gunter Meister

1. Berichterstatter: Prof. Dr. Gernot Längst

2. Berichterstatter: Prof. Dr. Matthias Mack

Tag der mündlichen Prüfung: 10.06.2022

Für Cäcilia Siegel

Abbreviations

° C	Degree Celsius
%	Percentage
~	Approximate
aa	Amino acid
approx.	approximately
ATP	Adensosine-5´-triphosphate
bp	Base pair
BSA	Bovine serum albumin
CHD	Chromodomain Helicase DNA binding domain
cm	centimeter
CoIP	Co-immunoprecipitation
d	Drosophila
Da	Dalton
DMSO	Dimethylsulfoxid
DNA	Deoxyribonucleic acid
dNTPs	2´-deoxynucleotide triphosphate
dox	Doxycycline
ds	Double strand
DTT	Dithiothreitol
EDTA	Ethylene amino tetra acetate
EGTA	Ethylen glycol tetra acetate
FCS	Fetal calf serum
g	Gram or acceleration of gravity
h	Hour or human
HDAC	Histone actetyl transferase
HEK	Human embryonic kidney
His	Histidine
IP	Immunoprecipitation
k	Kilo
l	liter
M	Molar
mA	Milliampere
MBD	Methyl-CpG-binding domain protein
min	Minute

ml	Milliliter
mm	Millimeter
mM	Millimolar
MS	Mass spectrometry
MSC	Mesenchymal stem cell
MTA	Metastasis-associated protein
µg	Microgram
µl	Microliter
ng	Nanogramm
nm	Nanometer
nM	Nanomolar
NuRD	Nucleosome remodeling and deactylation
PAA	Polyacrylamide
PI	Protease inhibitor
PHD	Plant homeodomain
RbAp	Retinoblastom binding protein
rpm	Revolutions per minute
RT	Room temperature
SDS	Sodium dodecyl sulfate
SDS-PAGE	Sodium dodecyl sulfate polyacrylamide electrophoresis
SF2	Helicase superfamily 2
SNF	Sucrose non fermenting
ss	Single strand
TEMED	N,N,N',N'-tetramethylethylenediamine
WB	Western Blot

List of figures

List of tables

1 Bilingual summaries

1.1 Summary

The eukaryotic cell has to organize its 2 m DNA into higher order structures to fit into the 10 µm nucleus. The DNA is associated with proteins and RNA to form the so called chromatin with its basic subunit the nucleosome, representing a 147 bp long B-DNA, wrapped 1.65x around a histone octamer. It is generally assumed that the nucleosome array is hierarchically folded in higher compaction levels. Active mechanisms exist that alter chromatin structure in order to retain its accessibility as well as intended inaccessibility. These dynamic modifications are crucial to the chromatin to regulate DNA accessibility to ensure DNA dependent processes like replication, transcription, or DNA repair. These dynamics are e.g. achieved by ATP dependent chromatin remodeling enzymes, which use the energy of ATP hydrolysis to translocate histoneoctamers along ds DNA. All active chromatin remodeler, shown so far, are members of the Snf2 family of the helicase Super Family 2 (SF2), classified by their similar ATPase domain. Two members of the Mi-2 subfamily, the ATPases CHD3 and CHD4 (Chromodomain, Helicase, DNA binding), are part of the multiprotein complex NuRD (Nucleosome Remodeling and histone Deacetylation). Misregulation or mutation of the chromatin remodelers CHD3 and CHD4 where shown to play a role in the pathogenesis of cancer or mesenchymal diseases like dermatomyositis. Remodelers are highly regulated in activity and by still badly characterized in mechanisms on specific genomic loci. This regulation can be achieved by interacting with distinct partners for example: Transcription factors.

Preliminary work of our lab showed an interaction of CHD3 and CHD4 with the myeloid and B-cell-specific transcription factor PU.1 *in vitro*. Here it is shown, that the interaction of the remodeling enzymes CHD3/4 and PU.1 also occur in context of living cells. We used in-house-made stably transfected HEK293 Flp-In™ T-Rex cells dox-inducible co-expressing either CHD3-GFP, CHD4-GFP and GFP with hPU.1-C-Myc-His. The cells were first verified by immunocytochemistry conductively showing sufficient inducible expression levels and correct localization of the proteins of interest. Second, the interaction of CHD3/CHD4-GFP and PU.1 was investigated by co-immunoprecipitation experiments by pulling down one interaction partner at a time followed in western blot analyses. We clearly could show an DNA-independent interaction between CHD3/CHD4-GFP and PU.1 and also in context of NuRD in the GFP-pulldown.

1.2 Zusammenfassung

Die eukaryotische DNA unterliegt aufgrund ihrer Länge von ca. 2 m komplexen Mechanismen, um eine Kompaktierung als sog. Chromatin im 10 µm großen Zellkern zu ermöglichen.
Die kleinste Untereinheit (UE) des Chromatin bildet das Nukleosom, bestehend aus 147 DNA-Basenpaaren, die sich 1,65x um ein Histonoktamer winden. Höhere DNA-Kompaktierungen bis hin zum Metaphasenchromosom erfolgen in Assoziation mit weiteren Proteinen sowie Ribonukleinsäuren. Um dabei eine adäquate Zugänglichkeit und v.a. Unzugänglichkeit für DNA-abhängige Prozesse wie DNA-Replikation, -Transkription und -Reparatur zu erreichen, ist ein stetiger und dynamischer Umbau des Chromatins nötig. Dieser erfolgt u.a. durch ATP-abhängige Chromatin Remodeling Enzyme.
Alle Chromatin Remodeler werden anhand ihrer ähnlichen ATPase-Domäne zur Snf2-Familie der Helicase Super Familie 2 (SF2) zusammengefasst. Sie verwenden die Energie aus der ATP-Hydrolyse, um die Nukleosome entlang der DNA zu repositionieren, sie zu entfernen oder einzufügen. Zwei Mitglieder ihrer Mi-2 Unterfamilie, CHD3 und CHD4 (Chromodomain, Helicase, DNA binding), sind zudem Bestandteil des NuRD-Komplex (Nucleosome Remodeling and histone Deacetylation). Werden sie fehlreguliert, führt dies zu einer Missverhältnis der DNA-abhängigen Prozesse und spiegelt sich in der Pathogenese verschiedener Tumore sowie Krankheiten wie der Dermatomyositis wieder. Daher ist eine strenge Regulation der Chromatin Remodeler essentiell. Dies geschieht z.B. durch Interaktion mit verschiedenen Transkriptionsfaktoren.
Vorangegangene Arbeiten unseres Labor konnten bereits eine *in vitro* Interaktion zwischen den beiden Chromatin Remodelern CHD3 und CHD4 mit dem myolischen B-Zell-spezifischen Transkriptionsfaktor PU.1 zeigen. Anknüpfend daran, wurden in dieser Studie stabil transfizierte HEK293 Flp-In™ T-Rex Zellen verwendet, die Doxyzyklin-induzierbar entweder CHD3-GFP, CHD4-GFP oder GFP zusammen mit hPU.1-C-Myc-His ko-exprimieren. Die hinreichende Proteinexpression sowie -lokalisation wurde mittels Immunhistochemie sowie Western Blot in einem ersten Schritt validiert. Anschließend wurde durch Co-Immunopräzipitationen (Co-IP) die Interaktion zwischen CHD3/CHD4-GFP und PU.1 analysiert. Dabei wurde jeweils ein Interaktionspartner präzipitiert und auf die Co-Präzipitation des anderen sowie NuRD-UEs untersucht. Wir konnten hierbei eine DNA-unabhängige Interaktion zwischen den Interaktionspartnern CHD3/CHD4-GFP und PU.1, sowie in Assoziation mit NuRD zeigen.

2 Introduction

2.1 Chromatin

The DNA comprises a total length of two meters constituting a major challenge for the cell to compress its size to fit into the 10 µm nucleus. Therefore a compaction by the factor of 200.000 is necessary to solve this issue (Längst and Becker 2004). The basic subunit of chromatin, the nucleosome, represents a right handed 147 bp long ds B-DNA, wrapped around a histone octamer consisting of two H2A/H2B dimers as well as one H3/H4 tetramer, respectively (Luger and Richmond 1998). The nucleosomes are connected via a 10 - 80 bp „linker DNA“. This results in a nucleosome array resembling a “bead on a string-structure” with 11 nm in diameter (Felsenfeld and Groudine 2003). To achieve even higher levels of compaction, the linker DNA is associated with a histone H1 on the entry and exit sites of the nucleosomes (Robinson et al. 2006).

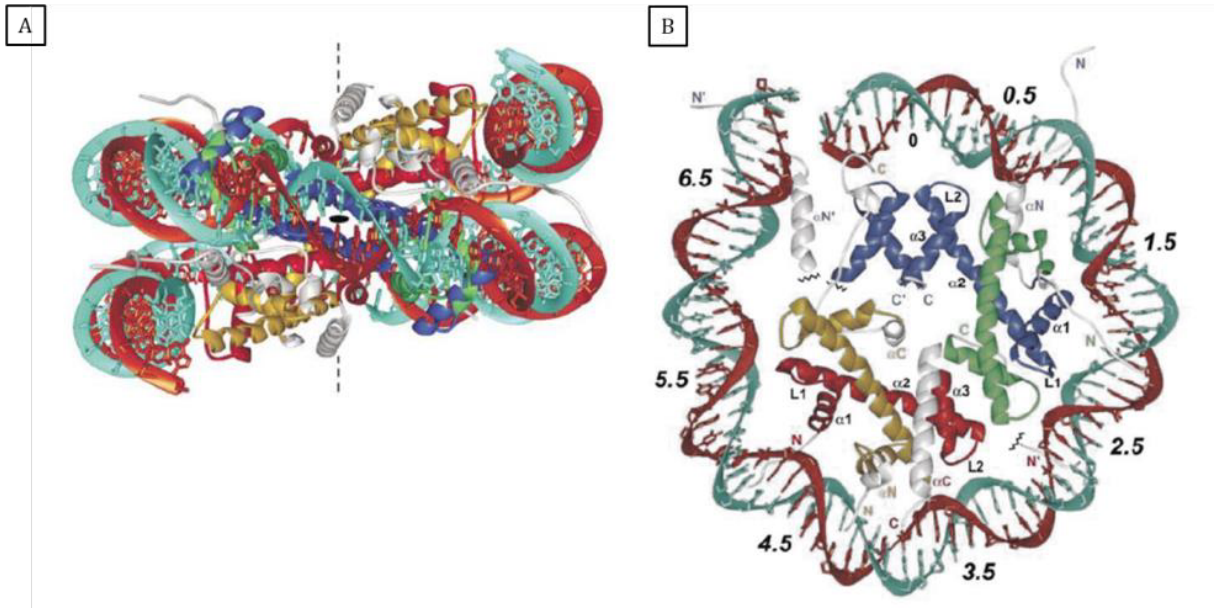

Figure 1: Nucleosome structure at 1.9 Å

View of nucleosome bundle (DNA in red and green). Histone proteins are shown in yellow (H2A), red (H2B), blue (H3) and green (H4). A: View down the axis of 2-fold pseudo-symmetry (dyad axis, black) with the DNA *superhelix* axis oriented vertically (broken line). B: Horizontal view through the a half nucleosome, to demonstrate the interaction of the DNA with the histones. Modified from (Davey et al. 2002)

Higher order structures of chromatin (Figure 2) and its mechanism are discussed controversially, with various theories being published. The solenoid model suggests that the nucleosomes are helical arranged with 6 nucleosomes per turn (Kruithof et al. 2009). Whereas the “zigzag-model” consists of a looser form of chromatin with irregular configuration

(Felsenfeld and Groudine 2003). Both theories lead to the 30 nm fiber (Woodcock and Ghosh 2010). Further levels of compaction between the 30 nm fiber and the well-studied metaphase chromosome, which represents the highest level of compaction, remain unclear (Felsenfeld and Groudine 2003). However, newer data argue against a regular compaction of chromatin (Eltsov et al. 2008; Fussner, Ching, and Bazett-Jones 2011).

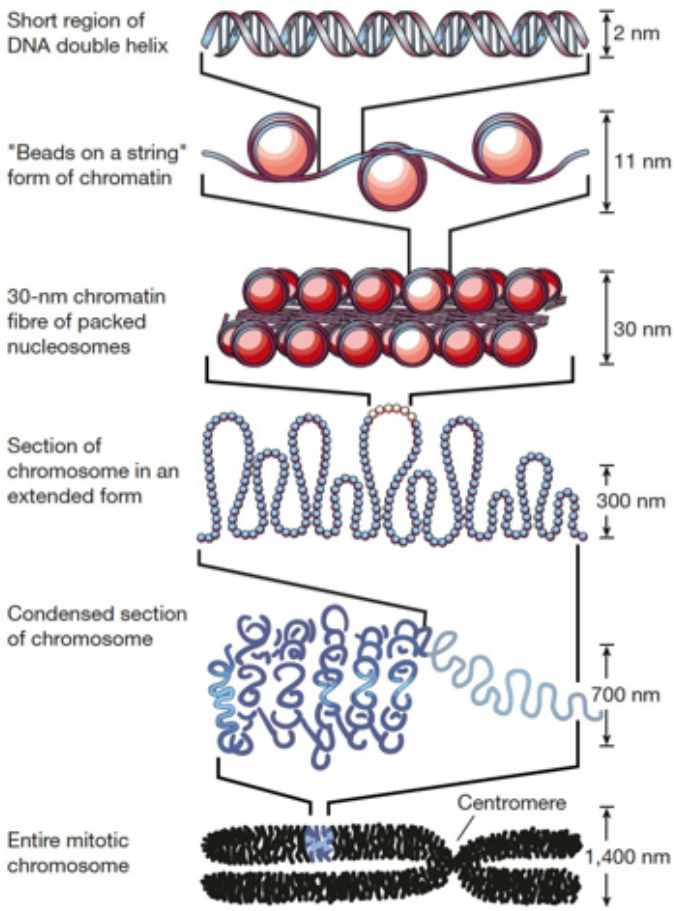

Figure 2: Chromatin compaction levels

Schematic overview of different packaging levels of the chromatin. The nucleosome represents its basic unit, which structure is also called “beads on a string”. The next compaction level, the 30 nm fiber, is suggested in two models. Further compaction levels are mainly speculative. The highest compaction level is the metaphase chromosome, which is again well documented. Modified from (Felsenfeld and Groudine 2003)

As the DNA in the nucleosome is inaccessible for transcription factors, higher order structures have to be opened and subsequently the octamers have to be either removed or moved along the DNA to enable TF binding. To guarantee a dynamic system, where the equilibrium between densely packed, inactive heterochromatin and the active and accessible euchromatin is regulated, constant remodeling of specific genomic regions is required. Processes like replication, transcription and DNA repair can only be executed in form of euchromatin. Therefore, it is emphasized, that the accessibility as well as the inaccessibility of DNA take part

in this regulatory processes (Felsenfeld and Groudine 2003). The machinery accomplishing these conversions are called chromatin remodelers.
Chromatin remodeling can occur at different levels: Post translational modification (PTM) of histones, incorporation of histone variants to the chromatin, DNA methylation and chromatin associated RNA (Bannister and Kouzarides 2011; Breiling and Lyko 2015; Greenberg and Bourchis 2019; Li and Fu 2019). A variety of mechanisms can be differentiated, where two are best examined. One of them mediates the interaction of the DNA with histones by covalent modification (Bannister and Kouzarides 2011), the other one relocates the octamers by ATP-depended hydrolysis (Becker and Hörz 2002).

2.2 Chromatin remodelers

All human chromatin remodelers share a similar domain of ATPases and are therefore classified into the SNF2 family within the SF2 superfamily (Flaus et al. 2006, Figure 3). The ATPase contains two tandem recA-like domains (Dexx and HELICc) with a variety of conserved helicase-related sequence motifs (Längst and Manelyte 2015). These enzymes use the energy of ATP hydrolysis to rebuild, modify and reconstruct the nucleosome structure (Becker and Hörz 2002; Saha, Wittmeyer, and Cairns 2006). This nucleosome dynamic is necessary to move, eject or restructure the composition and positions of octamers. Otherwise no proper transcription, replication or repair would be achievable (Clapier and Cairns 2009).

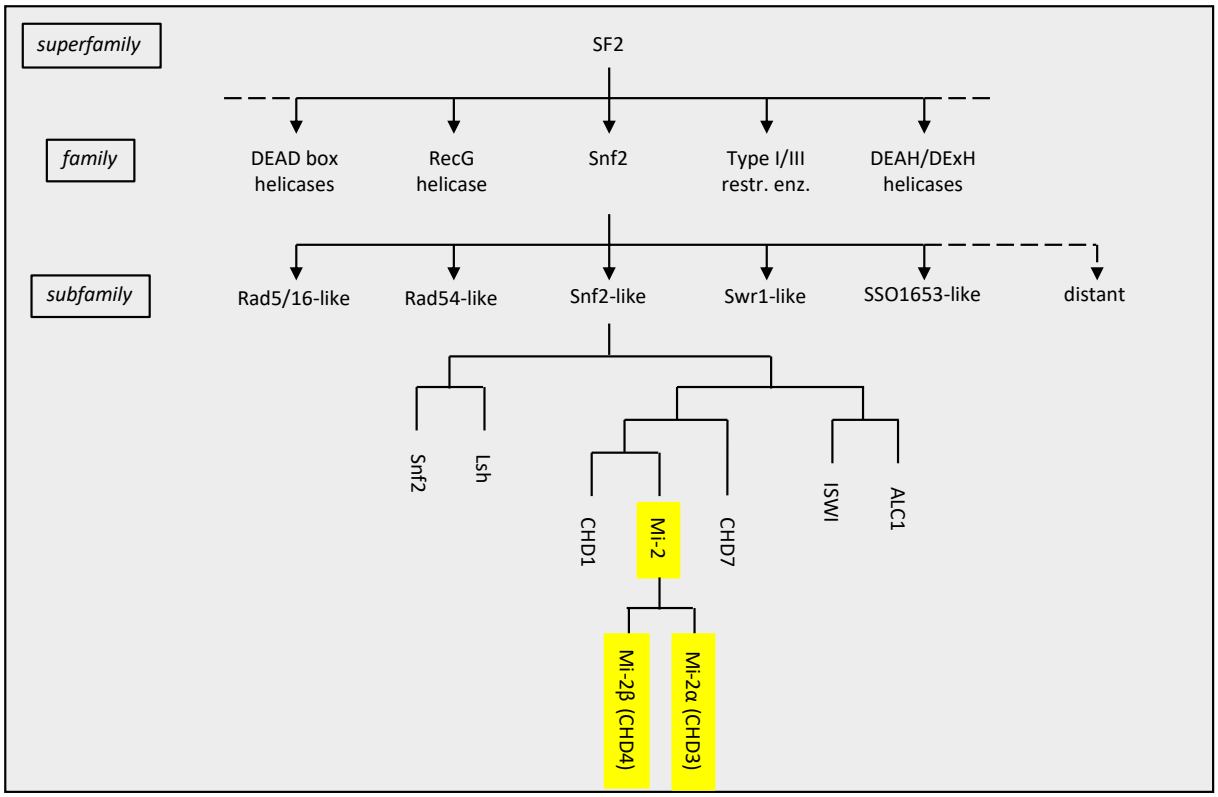

Figure 3: Hierarchical classification of DNA remodelers.

All chromatin remodeling enzymes belong to the Snf2 family. They are subsequently grouped in subfamilies. The Mi-2 members Mi-2α (CHD3) and Mi-2β (CHD4) are highlighted in yellow. Modified from (Flaus et al. 2006).

Differences in sequence and domains flanking the ATPase domain as well as their unique associated subgroups allow to mechanistically subgroup the chromatin remodelers (Clapier and Cairns 2009; Flaus et al. 2006). The best characterized are Snf2, ISWI and Mi-2. Snf2 (hBRG1) for example holds a HSA domain, which mediates intracomplex protein interactions, a SnAC and AT hook domain for DNA binding and a Bromodomain, which recognizes acetylated lysin residues in histon H3 and H4 tails. The function of the QLQ and BRK domain is still unknown. ISWI (Iswi1, Iswi2, Snf2h) contains a HAND, SLANT and Slide domain, which recognizes nucleosomes and internucleosomal DNA (Längst and Manelyte 2015). The Mi-2 proteins (CHD3/4) contain a tandem Chromodomain and a tandem zinc finger. Structure, function and substrates are described in the next chapter (2.2.1).

Chromatin remodeler share five basic properties: Their affinity to the nucleosome, a domain, which recognizes covalent histone modification, a similar ATPase domain, a domain regulating the ATPase domain and a domain for interaction with other proteins and chromatin factors (Clapier and Cairns 2009).

Several models for the mechanism of ATP dependent chromatin remodeling are critically discussed. Currently predominant is the “loop and recapture” model. The model suggests that the DNA-histone interaction are detached areas of the entry and exit site of the nucleosome.

The unbound DNA is pushed into the nucleosome creating a loop of approx. 10 bp propagating around the histone octamer (Längst and Becker 2004).

The chromatin remodeling enzymes usually exist in a variety of complexes. Various complexes can mediate a versatile set of effects to the same chromatin substrate. One essential representative of chromatin remodelers is hCHD3/hCHD4 (Mi-2 α/β) within the NuRD (**Nu**cleosome **R**emodeling and histone **D**eacetylation) complex. It was shown that its ATPase activity increases in context of the NuRD complex. This suggests a enhancing function of the complexes subunits to the effective ATPase activity (Xue et al. 1998).

2.2.1 Chromatin remodeling enzymes CHD3 and CHD4

Human (h) CHD3/CHD4 were first discovered as auto-antigens in dermatomyositis (Seelig et al. 1995) and characterized as negative regulators of gene expression in 1997 (Woodage et al. 1997). As like their drosophila analogue, dMi-2α (hCHD3) and dMi-2β (hCHD4), they belong to the Mi-2 subfamily of SNF2 helicase-like proteins (Figure *3*). CHD family members contain a tandem Chromo-domain (**Ch**romatin **O**rganization **Mo**difier **Domains**) and two PHD (**P**lant **H**omeo **D**omain) zinc fingers N-terminal to the conserved ATPase (Watson et al. 2012).
The Chromodomain was initially discovered in Drosophila heterochromatin protein 1 (HP1), which contains a single chromodomain. Initially suggested, the PHD domain is able to promote closed chromatin states and represses homoeotic genes during development (Ball et al. 1997; Pearce, Singh, and Gaunt 1992; Wreggett et al. 1994). Newer findings indicate that the primary function is to bind methylated histone residues. In case of CHD3 and CHD4 it interacts with the lysine residue 4 of histone H3 (H3K4) (Flanagan et al. 2005; Pray-Grant et al. 2005). It was shown that these domains have a preference for unmodified H3K4 and methylated H3K9 and are able to bind two histone H3 tails within one nucleosome (Mansfield et al. 2011; Musselman et al. 2009, 2012). In B-cell development this association plays a key-role in transcriptional repression (Musselman et al. 2012). For example, CHD4 exclusively binds to H3K4 and H3K9me3 but not H3K4me3, which mediates the transcriptional repression in context of NuRD (Mansfield et al. 2011; Musselman et al. 2012).
In comparison, CHD3 and CHD4 share an aa-sequence similarity of 71,6 %, but differ in the longer, unique C-terminus in CHD3 (Figure 4, Hoffmeister et al. 2017). The C-terminus of CHD3 was shown to interact with the interacting with Kap-1 corepressor (Figure 4, purple sequence).

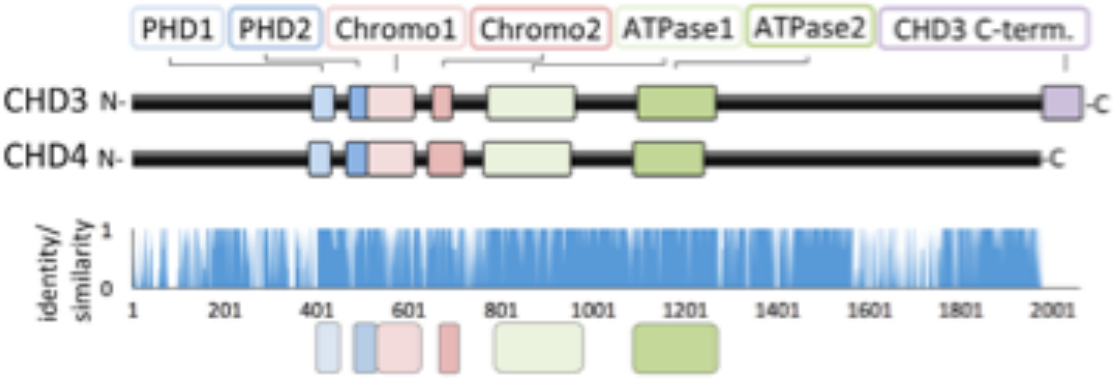

Figure 4: Comparison of hCHD3 and hCHD4

Upper panel: schematic comparison of hCHD3 (Uniprot Q12873) and hCHD4 (Uniprot Q14839) with their shared tandem PHD domains (blue), the common ATPase domains (green), as well as the two chromo domains (red). The hCHD3 specific C-terminus is shown in purple. Lower panel: hCHD3 and hCHD4 sequence alignment by Cluster Ω. Identical amino acids (aa) are presented with value 1, highly similar aa with 0,66, weakly similar aa with 0,33 and different aa with 0. (Hoffmeister et al. 2017)

2.2.2 The chromatin remodeling complex NuRD

In 1998 the NuRD complex was initially described as a transcriptional repressor, because of its subunits, e.g. MBD 2/3. Notably at this point, this complex combines uniquely two enzymatic activities compared to other complexes known: ATP-dependent nucleosome remodeling and histone deacetylation (Tong et al. 1998; Wade et al. 1998; Xue et al. 1998; Y. Zhang et al. 1999). It is highly conserved from plants to animals with a wide range of expression in developing or mature tissues (Denslow and Wade 2007). It comprises at least 6 so called core proteins, which can be subdivided into enzymatic and non-enzymatic subunits. (1) **H**istone **d**e**ac**etylase 1/2 (HDAC1/2) and (2) a CHD protein (accordingly CHD3 or CHD4) belong to the enzymatic subunits. The non-enzymatic members of NuRD are: (3) MBD2/3 (**M**ethyl-CpG-**b**inding **d**omain protein), (4) MTA1/2/3 (**M**etas**t**asis-**a**ssociated protein), (5) RBBP4/7 (**R**etino**b**lastom **b**inding **p**rotein, also known as RbAp 46/48) and (6) the nuclear zink-finger proteins GATAD2A & GATAD2B (also known as p66α/β).

The enzymatic subunits CHD3/4 with its ATPase can assemble, move or eject nucleosomes, while HDAC1/2 deacetylates lysine residues of histone tails or other proteins like p53 (Gururaj et al. 2006). MBD2/3 can bind cytosine-methylated DNA (Hashimoto et al. 2012; Hendrich and Bird 1998). MTA1/2/3 mediates the binding between the complex and DNA as well as to

HDAC1 and is also able to interact with other transcription factors (Fujita et al. 2003; Hendrich and Bird 1998; Hong et al. 2005; Roche et al. 2008). RbAp 46/48 acts as a scaffolding protein, coordinating the assembly of the multi-protein complex and binds histone H4 (Murzina et al. 2008). p66 α/β build a coiled-coiled antiparallel interface with MBD2/3, which connects both Core deacetylase complex and Chromatin remodeling submodule (Figure 5, black arrow) (Basta and Rauchman 2017).

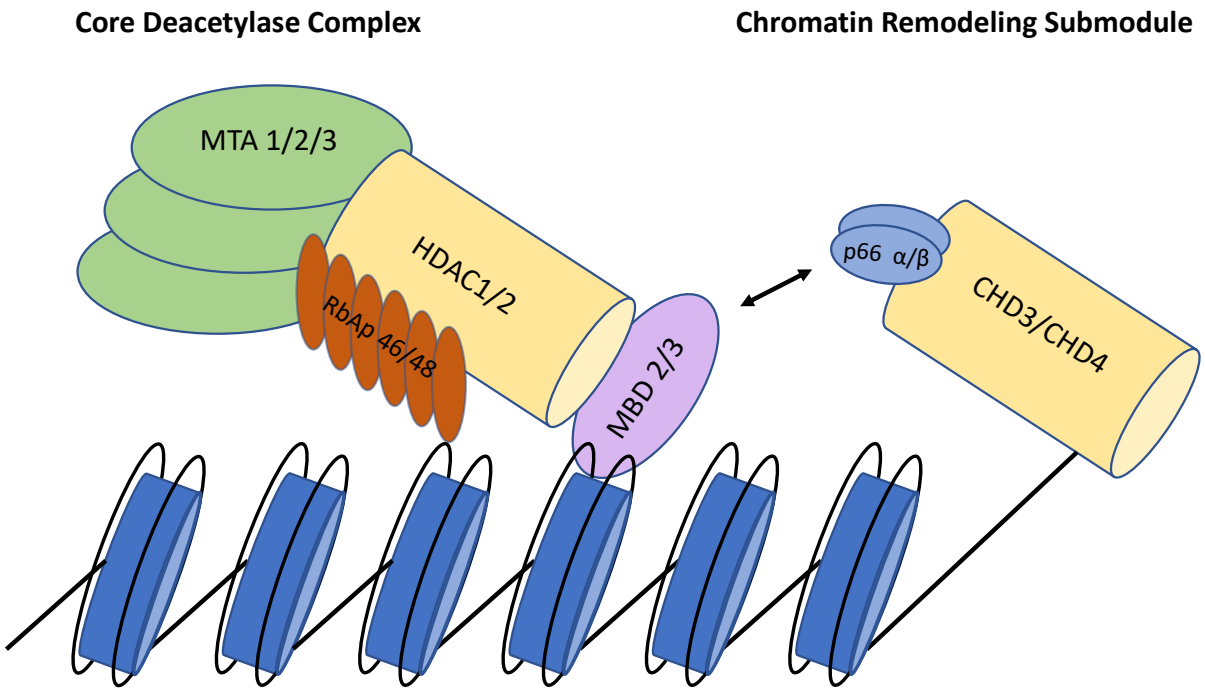

Figure 5: Architecture and assembly of the NuRD complex.

The assembly of the NuRD complex is divided in the deacetylase complex and the chromatin remodeling submodule. The Core deacetylase complex contains the MTA1/2/3, HDAC1/2, RbAp46/48 and MBD2/3 subunits. The chromatin remodeling submodule consists of Mi2 (CHD3 or CHD4 respectively) and p66 α/β. (Modified from Basta and Rauchman 2017)

Also, post translational modifications (PTMs) of NuRD components take influence on its functional behavior. E.g. if MTA1 is methylated on its lysine residue 532, it causes an repressive effect on gene transcription (Nair, Li, and Kumar 2013). This can be explained by the higher affinity of methylated MTA1 on histone H3 resulting in H3K9me state and recruitment of CHD4 for a repressive chromatin environment. In case of demethylation of MTA1, CHD4 and therefore NuRD is displaced, which results in the activation of gene transcription (Nair, Li, and Kumar 2013; Si et al. 2015).

By now, Hoffmeister et al. also showed that NuRD does not only function as an repressor but also as an activator for transcription (Hoffmeister et al. 2017). Multiple subunits of NuRD can interact either with DNA directly or histones to regulate gene expression and genome integrity.

As mentioned above, either one CHD3 or one CHD4 protein is part of the NuRD complexes (Hoffmeister et al. 2017). They are co-expressed in many human tissues, suggesting even if they share this high similarity, CHD3 and CHD4 act in distinct roles in cell environment and multi-protein-complexes (Tong et al. 1998).

2.3 Transcription factors in gene expression

The human genome contains about 20’000 protein-coding genes occupying about 25 % of the 3 billion bp. Even though every cell shares the same DNA, the cells must be capable of expressing tissue specific and differentiation status depending proteins besides the ubiquitous needed proteins (Eeckhoute, Métivier, and Salbert 2009). To get there, the standard human transcription machinery has to be regulated. This is achieved by the cooperation of certain transcription factors, which can be divided in general and specific transcription factors.
By default, the machinery consists of the RNA Polymerase II (RNA Pol II) and general transcription factors, which are necessary for all RNA Pol II Promotors, the TBP (TATA-Box binding protein) and TFIIB (Transcription factor B (also known as preinitiation complex (PIC). General transcription factors are ubiquitous in the human cells and help the RNA Polymerase II (RNA Pol II) to correctly bind the promoter. Together they create a 2 MDa complex, which assembles on the core promotor, comprising the TATA-box, the BRE-element (Transcription factor B Recognition element) and the INR-element (Initiator) (Hausner and Thomm 2001).
The basal procedure of gene expression starts, when intra or extracellular receptors are stimulated. This stimulation initiate a signal cascade, leading to recruitment and activation of transcription factors (TFs), e.g. the general TFIIA-H, which bind in tandem with the PIC at the core-promotor. Together they build the Initiation complex. The process has to be tightly regulated and therefore a subset of specific TFs is required (Buratowski 1994).
Specific transcription factors are important in the cell type specific gene expression. Depending of their particular structure, they directly bind the DNA, the RNA Pol II or recruit other transcription factors in the promoter or enhancing regions.
Firstly described in 1980, TFs included any proteins, that are involved in transcription or altering gene expression levels (Johnson and McKnight 1989). Nowadays, they are defined by the ability to bind a specific DNA sequence and regulate transcription (Fulton et al. 2009; Vaquerizas et al. 2009). They can be classified by their binding motifs: Zinc-finger, Helix-turn-Helix-, Helix-Loop helix, leucin-zipper- or winged-helix motifs constitute about 80 % of all TFs. Even more binding motifs are discovered since (Lambert et al. 2018). Binding to their specific DNA-sequences mark the crucial basis in regulating gene transcription. Typically,

these sequences are 5-15 bp in length and can be divided in cis- and trans-acting elements. Cis-acting sequences includes regulatory motifs located nearby or right adjacent to the gene, modifying the accessibility in chromatin environment. Trans-acting elements are sequences, which are located far away of the gene and work either to initiate, enhance or suppress gene expression. This is achieved e.g. by looping the DNA.
It's a big aim for modern research to clarify how a limited set of TFs is able to regulate a variety of multiple tissues in differentiation or homeostasis. In addition, the same TFs can regulate different genes in different cell types (Gertz et al. 2012).
A complex system of regulatory mechanism enables a dynamic gene expression and thus, a high variety within one organism (Lambert et al. 2018). Failure in this highly coordinated system can cause diseases, which remains a research target to exogenous modify this.

2.3.1 The specific transcription factor PU.1

PU.1 is expressed exclusively in hematopoietic cells, with high protein levels in monocytes, granulocytes and B-lymphoid cells (Chen et al. 1995; Goebl 1990; Hromas et al. 1993; Klemsz et al. 1990; Moreau-Gachelin, Tavitian, and Tambourin 1988). Firstly identified as a protein that binds purin-rich-sequences (PU-box), it was further described as a master regulator in hematopoiesis and immune response (Friedman 2007). PU.1 is expressed in CMPs, its expression levels increase in GMPs and decrease in megakaryocyte-erythrocyte progenitors (Akashi et al. 2000; Chen et al. 1995; Hromas et al. 1993; Klemsz et al. 1990; Miyamoto et al. 2002). In mature cells, Pu.1 is predominantly expressed in the macrophagous linage, but less in B-cells. It modulates immunoglobulin genes and macrophage colony stimulation factor (M-CSF) (Nelsen et al. 1993). When the PU.1-expression is downregulated during differentiation, γ-ray treatment or during proviral integration, the cells show a misregulation of PU.1 that causes leukemia (M. K. Anderson et al. 1999; Michele K. Anderson et al. 2002; Cook et al. 2004; Miyamoto et al. 2002; Moreau-Gachelin 1994). The regulation of PU.1 occurs through phosphorylation of serine residues as well as interaction with other factors like TFIID GATA1/2 or posttranscriptional via miRNAs (Burda, Laslo, and Stopka 2010). In addition, McKercher and Scott showed that a complete knockout of PU.1 in mice causes embryonic or postnatal death, which can be traced back to a lack of macrophages, granulocytes and B-/T-cells (McKercher et al. 1996; Scott et al. 1994).
Belonging to the ETS-family (**E**26 **t**ransformation-**s**pecific) of specific transcription factors, PU.1 (purin-rich box 1) is membered in the subfamily of SP1-proteins (Klemsz et al. 1990;

Moreau-Gachelin 1994). The ETS-family is defined through its highly conserved DNA-binding ETS domain and further subgrouped by additional domains and phosphorylated groups (Hollenhorst, McIntosh, and Graves 2011). ETS-family members regulate a variety of genes in combination with other TFs like SP1 (specifity protein 1), RUNx1 (run-related transcription factor 1) or CEBP (CCAAT/enhancer binding protein).

PU.1 has a winged-helix-turn-helix (wHTH domain with three α-helices (α1-α3) and four β-sheets (β1/β4), with the third α-helix binding the DNA (Donaldson et al. 1996). The protein consists of three functional domains: (a) a C-terminal ETS-binding domain, which is able to bind DNA and interact with other proteins (Behre et al. 1999; Nerlov et al. 2000; Rekhtman et al. 1999). It recognizes a purin-rich GGAA/T-sequence (PU-box), but its specificity may also occur through its adjacent nucleotides (Wei et al. 2010). (b) A N-terminal transactivation domain (TAD), which occurs as glutamine-rich region. This domain interacts with TFs like TFIID, TBP, TATA-associated factors (TAFs) and also GATA1/2 (Hagemeier et al. 1993; Nagulapalli, Pongubala, and Atchison 1995; P. Zhang et al. 2000). By interacting with TBP and TAFs, PU.1 is able to recruit and stabilize the default transcription machinery. In between these two domains, PU.1 harbours (c) a PEST-domain. The name is composed of the amino acids dominantly appearing in this domain: prolin (P), glutamic acid (E), serine (S) and threonine residues (T). It interacts with interferon regulatory factors (IRFs) (Eisenbeis, Singh, and Storb 1995; Pongubala et al. 1993; Pongubala and Atchison 1997). In 2000, Zhang could show that the ETS domain of PU.1 is able to interact with the Zn-finger of GATA1 (P. Zhang et al. 2000), which led to speculation if it can interact with other Zn-finger motifs. Our lab could previously show that NuRD, more precisely the catalytic motor proteins CHD3/4 alone can interact with the myeloid and B-cell-specific transcription factor PU.1 *in vitro* (Hoffmeister et al. 2017).

2.4 Aims of the study

Preliminary work of Andreas Fuchs and Nadja Tedesco (both this lab, not published yet) showed that hCHD3 and hCHD4 directly interact with hPU.1 and DNA independent *in vitro*. In addition, it could be demonstrated that PU.1 opposingly regulates the remodeling and ATP hydrolysis of CHD3 and CHD4 *in vitro*. Studies with THP cells expressing PU.1 upon differentiation to macrophages could not prove this interaction in vivo, since the studied interaction partners were not expressed at sufficient levels for detection. Furthermore, in terms of practicability cultivating and differentiating THP cells was time consuming and cost intensive.

Therefore, we decided to generate stably transfected HEK293 cells, dox-inducible co-expressing either CHD3-GFP/PU.1-C-Myc-6xHis, CHD4-GFP/PU.1-C-Myc-6xHis or GFP/PU.1-C-Myc-6xHis. The established cell lines had to be basic characterized to verify the precise expression and localization of the proteins of interest. To clarify a DNA-independent interaction between PU.1 and CHDs in context of living cells, we used Co-immunoprecipitation (Co-IP) experiments pulling down either their GFP- or Myc-tag, subsequently analyzed by western blot.

3 Material & Methods

3.1 Material

3.1.1 Water

The used water was purified with PURELAB Ultra ion exchange system. It has an electrical resistance of 18,2 MΩ/cm. Hereinafter this water was used whenever "water" or H_2O is mentioned. For less critical work, deionized water from the university's ion exchanger was utilized.

3.1.2 Chemicals

Common chemicals and solutions are shown in Table 1 .

Name	**Supplier**
Acetic acid	Fluka
Ammonium persulfate	Sigma-Aldrich corporation
Blasticidin 10 mg/ml	Life Technologies corporation
blocked agarose beads (Cat. No. bab-20)	ChromoTek GmbH
Bradford reagent	BioRad
Bromphenol Blue	Sigma-Aldrich corporation
BSA 10 mg/ml	New England Biolabs
complete, EDTA-Free; protease inhibitor cocktail	F. Hoffmann-La Roche AG
Coomassie Brilliant Blue G-250	Bio-Rad Laboratories, Inc
DMEM, Low Glucose, GlutaMAX™, Pyruvate	Life Technologies corporation
Doxycycline	Clontech/Takara Bio Company
DTT	Carl Roth GmbH + Co. KG
EDTA	Merck KGaA
EGTA	Sigma-Aldrich corporation
Ethanol tech./p.A	Sigma-Aldrich corporation
Ethidium bromide	Carl Roth GmbH + Co. KG
GFP-TRAP_A beads (Cat. No. gta-200)	ChromoTek GmbH
Glycerol	Carl Roth GmbH + Co. KG
Glycine	Sigma-Aldrich corporation
HCl 37 %	VWR

Hygromycin B 50 mg/ml	Life Technologies corporation
IGEPAL CA-630	Sigma-Aldrich corporation
Isopropanol p.A.	VWR
KCl	Labochem
KH_2PO_4	Sigma-Aldrich corporation
Laboratory film	Parafilm
Methanol p.A.	VWR
$MgCl_2$	Merck KGaA
Myc-Trap Agarose (Cat. No. yta-20)	Carl Roth GmbH + Co. KG
N,N,N',N'-Tetramethylethylendiamin (TEMED)	Carl Roth GmbH + Co. KG
Na_2CO_3	Riedel deHäen
$Na_2S_2O_3$ x 5 H_2O	Riedel deHäen
NaCl	Fisher chemicals
Rotiphorese® Gel 30	Carl Roth GmbH + Co. KG
Skim milk powder	Sucofin
TET-free Foetal Bovine Serum	Pan Biotech
Tris	Carl Roth GmbH + Co. KG
Tween	Carl Roth GmbH + Co. KG
Waterfree Na_2HPO_4	Sigma-Aldrich corporation

Table 1: Chemicals

3.1.3 Consumables

Name	**Supplier**
Cell culture dish P10 cell+	Sarstedt AG & Co
Cell culture dish P150 cell+	Sarstedt AG & Co
Cell culture flask T175 cell	Sarstedt AG & Co
Cell culture flask T25 cell	Sarstedt AG & Co
Cell culture flast T75 cell	Sarstedt AG & Co
cell culture plate 24 well cell+	Sarstedt AG & Co
Cell culture plate 6 well cell+	Sarstedt AG & Co
Cryo Vials	Nunc A/S
Falcon tubes (15 ml, 50 ml)	Sarstedt AG & Co
Gel cassettes 1 mm	Life Technologies corporation
Glass cover slips	Carl Roth GmbH + Co. KG/VWR
Low bind 5 ml tube	Eppendorf
Low bind reaction tubes 1.5 ml	Sarstedt AG & Co
Pipette tips (filtered) 10 µl; 20 µl; 200 µl; 1000 µl	Sarstedt AG & Co
Pipette tips 10 µl; 20 µl; 200 µl; 1000 µl	Sarstedt AG & Co
Plastic cuvettes	Sarstedt AG & Co

PVDF membrane	Millipore/ Merck KGaA
Reaction tubes 1.5 ml; 2 ml	Sarstedt AG & Co
Scrubber	Sarstedt AG & Co
Serological pipettes 2 ml; 5 ml; 10 ml; 25 ml, 50 ml	Sarstedt AG & Co
Syringes	BD Biosciences
Whatman paper 0.36 mm	Macherey-Nagel

Table 2: Consumables

3.1.4 Technical devices

Name	**Application**	**Supplier**
-20 °C, 4 °C refrigerator	Refrigerator	Generic household appliance
-80 °C freezer	Freezer	SANYO Electric Co., Ltd.
Novex XCell SureLock Mini-Cell	Mini SDS gels	Life technologies corporation
XCell4SureLock™ Midi-Cell	Midi SDS gels	Thermo scientific
Pipetboy comfort	Electric pipetting aid	IBS Integra Bioscience
Pipettes (10 µl, 20 µl, 200 µl, 1000 µl)	Pipettes	Gilson, Inc.
Semi dry electro blot system	Blotting system	Bio-Rad Laboratories, Inc
Unigeldryer 3545D	Gel dryer	Uniequip
Tabletop centrifuge	Centrifuge	Roth
Centrifuge 5415 R	Centrifuge	Eppendorf AG
EPS301	Electrophoresis power supply	Amersham Biosciences
Biorupter ® Standard	Sonifier	Diagenode
Ultrospec 3100 pro	Spectrophotometer	Amersham Biosciences
Axiovert 200M	Fluorescence Microscope	Carl Zeiss AG
Purelab Ultra	Water purification system	ELGA LabWaters VWS
REAX Top	Vortexer	Heidolph
Polymax 1040	Platform shaker	Heidolph
Incubator	Incubator	HT Infors
Perfection V700	Photo Scanner	Seiko Epson Corporation
pH meter	pH meter	Knick
Safe Imager System	Imager	Life technologies corporation
CO_2 incubator	Mammalian cell Incubator	SANYO Electric Co., Ltd.
Fluorescence Image Reader FLA-3000	Imager	Fujifilm Holdings Corporation

Table 3: Technical devices

3.1.5 General buffers and solutions

Buffer	Component	Concentration	Amount
10 x PBS	NaCl		400 g
	KCl		10 g
	Waterfree Na_2HPO_4		72 g
	KH_2PO_4		12 g
	H_2O		Ad 5 l and titrate to pH 7.4
EDTA	EDTA	0.5 M	18.612 g
	H_2O		Titrate to pH 8.0 (~2 g NaOH) Ad 100 ml
EGTA	EGTA	0.5 M	19.0175 g
	H_2O		Titrate to pH 8.0 (~4 g NaOH) Ad 100 ml
EX0 +/- glycerol	1 M Tris-HCl pH 7.6	20 mM	10 ml
	1 M $MgCl_2$	1.5 mM	750 µl
	0.5 M EGTA	0.5 mM	500 µl
	99 % glycerol	10 %	50 ml
	H_2O		Ad 500 ml
EX1000 +/- glycerol	1 M Tris-HCl pH 7.6	20 mM	10 ml
	1 M $MgCl_2$	1.5 mM	750 µl
	0.5 M EGTA	0.5 mM	500 µl
	99 % Glycerol	10 %	50 ml
	KCl	1000 mM	37.3 g
	H_2O		Ad 500 ml
$MgCl_2$ * 6 H_2O	$MgCl_2$ * 6 H_2O	1 M	20.33 g
	H_2O		Ad 100 ml
Protease inhibitor solution		Use 1:50	1 tablet in 1 ml H_2O
Sodium azide	Sodium azide Use 1:100	10 %	
10 x SDS electro-phoresis buffer	Glycin	2 M	334 g
	Tris	250 mM	30,3 g
	SDS	1 %	10 g
	H_2O		Ad 1 l

Table 4: General buffers and solutions

3.1.6 Kits

Name	Supplier
BM Chemiluminescence Blotting Substrate (POD)	Roche applied science
SuperSignal West Dura Extende Duration Substrae	Thermo Scientific
Supernova Westar Substrate	Cyanagen

Table 5: Kits

3.1.7 Software

Name	Version	Supplier
Microsoft Word	Version 16.25	Microsoft Corporation
Microsoft Excel	Version 16.25	Microsoft Corporation
Multi Gauge	V 3.0	Fujifilm Holdings Corporation
Epson Scan	n.a.	Seiko Epson Corporation
Axiovison	Rel. 4.7	Carl Zeiss AG
Adobe Photoshop	CS 5 & CS 6	Adobe Systems Inporporated

Table 6: Software

3.1.8 Antibodies

Name	Species	Application	Source
Anti-PU.1 (sc-352)	Rabbit	WB	Santa Cruz Inc.
Anti-Lamin A/C (sc–20681)	Rabbit	WB	Santa Cruz Inc.
Anti-HDAC1 (sc-7872	Rabbit	WB	Santa Cruz Inc.
Anti-MTA2 (ab-8106)	Rabbit	WB	Abcam plc.
Anti-RbAp 46 (ab-3535)	Rabbit	WB	Abcam plc.
Anti-Mi2 (sc-11378)	Rabbit	WB	Santa Cruz Inc.
Anti-GFP (3H9)	Rat	WB	ChromoTek GmbH
Anti-C-Myc (9E10) (sc-40)	Mouse	WB	Santa Cruz Inc.
Anti-CHD3_A		WB	Alil
Anti-CHD3_N		WB	Prof. Dr. Weidong Wang, National Institute on aging, Baltimore, Maryland

Anti-CHD4_N		WB	Prof. Dr. Weidong Wang, National Institute on aging, Baltimore, Maryland
Anti-6x-His (ab9108)	Rabbit	WB	Abcam plc.
Anti-Penta His (34660)	Mouse	WB	Qiagen N.V.

Table 7: Antibodies

Secondary antibodies for western blots were used from Tschochners Lab, with the internal numbers #78 (anti rabbit), #79 (anti mouse) and #80 (anti rat) and #93 (Alexa 594, anti-mouse)

3.1.9 Mammalian cells

HEK293 T-Rex Flp-In™ were used to investigate the interaction between CHD3/CHD4 and PU.1 in the context of NuRD, in living cells. Therefore Hek TRex™ cells stably expressing Dox-inducible CHD3-GFP, CHD4-GFP or GFP alone (Andreas Fuchs, Masterthesis) were again stably transfected with constructs, encoding Dox-inducible hPU.1-C-Myc-His (done by Helen Hoffmeister and Elisabeth Silberhorn, both this lab).

Cell line	**Description**	**Culture properties**	**Source**
HEK293 TRex Flp-In + hCHD3-C-GFP + hPU.1-C-Myc-His	Human embryonic kidney cells	Adherent cells	Helen Hoffmeister, Elisabeth Silberhorn, Andreas Fuchs
HEK293 TRex Flp-In + hCHD4-C-GFP + hPU.1-C-Myc-His	Human embryonic kidney cells	Adherent cells	Helen Hoffmeister, Elisabeth Silberhorn, Andreas Fuchs
HEK293 TRex Flp-In + GFP + hPU.1-C-Myc-His	Human embryonic kidney cells	Adherent cells	Helen Hoffmeister, Elisabeth Silberhorn, Andreas Fuchs

Table 8: Mammalian cell lines

In the following, the cell lines are only termed CHD3-GFP, CHD4-GFP and GFP in order of Table 8.

3.2 Methods

3.2.1 Mammalian cell culture

3.2.1.1 Culturing cells

Components	Supplier
DMEM low glucose Glutamax	Life Technologies Corp™
TET-free FCS	Pan Biotech
Blasticidine	Life Technologies corporation
Pyromycin	Life Technologies corporation
Hygromycin	Life Technologies corporation

Table 9: Medium and supplements for HEK293 cells

HEK 293 cells were cultivated in DMEM low glucose Glutamax (Life Technologies Corp™). 500 ml medium were supplemented with approx. 48 ml TET-free FCS (final concentration 9,6 %), 10 µg/ml blasticidine, 100 µg/ml hygromycin and 500 ng/ml pyromycin. The cells were cultured at 37° C and 5 % CO_2 in a fully saturated atmosphere. For expanding, the cells were cultivated in T175 flasks first. Depending on the henceforth experiments, the confluent cells were split in 150 mm, 100 mm plates or 6-12 well plates. C+ type culturing vessels (Sarstedt®) were used. HEK 293 cells were splitted every two to three days. For splitting, cells were trypsinized in 1x trypsin for 3 minutes in the incubator. After that, trypsinazation was stopped with the 4-5 x amount of medium. The suspension was then partitioned into the required cell density. All cell culture tasks were performed in a laminar flow bench.

3.2.1.2 Freezing cells

HEK 293 cells were trypsinized and resuspended in DMEM low glucose Glutamax (Life Technologies Corp™) with FCS, followed by centrifugation at 650 g at RT for 5 minutes. Subsequently the pellets were resuspended in antibiotic free DMEM low glucose Glutamax (Life Technologies Corp™) with FCS and 8% DMSO. The suspension was aliquoted in 1 ml cryo-vials and immediately transferred in a -20° C pre-cooled cryogenic vessel and put into a - 80° C freezer. Depending on the cell density, 3 – 4 cryo-vessels were generated out of one confluent T175 flask.

3.2.1.3 Thawing cells

The almost thawed cell suspension of one vial was resuspended in 12 ml warm antibiotic-free DMEM low glucose Glutamax (Life Technologies Corp™) medium with FCS to dilute immediately the DMSO concentration. The cells were cultivated in T25 flasks. With increasing adherence, the medium was changed the next day or latest two day later and supplemented, with 10 µg/ml blasticidin, 100 µg/ml hygromycin and 500 ng/ml pyromycin.

3.2.1.4 Fluorescence microscopy of mammalian cells-Immunocytochemistry

	Component	Amount
4 % Para-Formaldehyde (PFA)	10 x PBS	10 ml
	Para-Formaldehyde	4 g
	1 M NaOH	1 drop
	1 M HCl	Titrate to pH 7,4
	H_2O	ad 100 ml

Table 10: Recipe for 4 % PFA

For fluorescence microscopy the cells were cultivated on cover slips either in Ø 35 mm plates or 6 well plates. At 50-70 % confluency, the cover slips were either treated with DMEM low glucose Glutamax (Life Technologies Corp™) supplemented with FCS (see 3.2.1.1) and 1 ng/µl doxycycline or with antibiotic-free DMEM low glucose Glutamax (Life Technologies Corp™) with FCS (see 3.2.1.1) for 24 h. Then, the cells were fixed in 4 % PFA/PBS for 15 min at RT. The cells were washed three times with PBS and subsequently treated with 0,25 % Triton X-100 for 30 minutes at RT. Again, the cells were washed three times with PBS followed by a blocking step with 2 % BSA/PBS for 1 h at RT. Afterwards, the cells were stained upside-down on a 50 µl drop of a 1:2 diluted Anti-myc 9E10 antibody (2 % in BSA/PBS) in a dark and humid environment for 1h at RT. After three washing steps with PBS, the cells were treated with an Alexa594 coupled secondary antibody (anti mouse, diluted 1:500 in 2 % BSA/PBS) under the same conditions. The cells were washed three times with PBS. Subsequently, the cells were DAPI stained (50 ng/ml in PBS) for 3 minutes at RT. Cells were washed three times with PBS and mounted face up on a glass slide, immersed in 50 % glycerol/PBS. A 10 x 40 mm cover slip was attached on top. Cells then were examined using a Zeiss Axiover 200 fluorescence

microscope with 63x oil enlargement. The images were documented using Zeiss Axiovision Rel. 4.7 software.

3.2.1.5 Preparation of Whole Cell Extract (WCE)

Cells were harvested 24 h after induction with 1 ng/µl doxycycline at ~ 70% confluency by scraping. Cells of three 150 mm plates were collected in one 50 ml Falcon tube respectively and centrifuged at 4500 rpm (Centrifuge 5415R, Eppendorf AG) for 10 minutes at 4° C. For the basic characterization of the cell lines, non-induced cells were proceeded under the same conditions.

After centrifugation, the supernatant was discarded and the pellets were resuspended in 1x PBS and transferred into a 1,5 ml reaction tube (Eppendorf®). Centrifugation was repeated at 1600 g for 10 minutes at 4° C, followed by remove of the supernatant. Depending on the current need of cells, the pellets were either frozen by shock freezing in liquid nitrogen with subsequent storage at -80° C or directly lysed with lysis buffer (see Table *11*), using 100 µl lysis buffer per cell pellet (out of 2x150 mm plates). Depending on the required amount of cell extract, two or more 150 mm plates were lysed. The pellet was incubated with lysis buffer for 10 minutes on ice followed by a sonication step in a Diagenode Bioruptor® for 5 minutes (power: high, duty circle: 30 s on, 30 s off). The water in the Biotruptor was cooled by putting approx. 80 g crushed ice into it. After that, the lysates were centrifuged with 16000 g for 10 minutes at 4° C. The protein concentration of the supernatant was measured by Bradford assay and represented the so called WCE (Whole cell extract) (see 3.2.2.1).

Name	Component	Concentration	Amount
Cell lysis buffer	EX 0 + glycerol	150 mM	3645 µl
	EX 1000 + glycerol		750 µl
	1 M DTT	3 mM	5 µl
	10 % IGEPAL CA-630 in H_2O	0,5 % (v/v)	500 µl
	PI-solution	1 %	100 µl

Table 11: Recipe for cell lysis buffer

3.2.2 Protein methods

3.2.2.1 Bradford assay

Bradford assay was performed to measure protein concentrations (Bradford 1976). Bio-Rad Protein assay-Reagent was diluted 1:5 in H_2O and 1 ml of it was given into the cuvettes. Either 10 µl BSA (Concentrations: 0.0, 0.1, 0.25, 0.5, 1.5, 5.0 µg/µl), for calibration, or 2 µl lysate sample was added. There was always a buffer control of 2 µl to determine any interferences. Before measuring the absorbance at 590 nm and 450 nm, the photometer was blanked with H_2O. The quotients of A590/450 nm were calculated. To get the „corrected A590/450“ quotient, ”BSA 0 µg/µl “quotient was subtracted from all quotients. Every amount of BSA of the calibration curve was divided through its corresponding and „corrected A590/450“ quotient.
The „corrected A590/450“ of measured protein samples were multiplied with the average of the calibration curve to receive the total protein amount. If it occurred that one value was out of range, it was eliminated. To receive the concentration per µl, the total amount was divided through the measured volume. All calculations were performed in Microsoft Excel.

Buffer	Component	Concentration	Amount
Tris-HCl	Tris	1 M	121.14 g
(pH 6.8, 8.8)	HCl 37 %		Titrate to desired pH
	H_2O		Ad 1 l
4 x lower Tris buffer	Tris	1,5 M	181,71 g
	HCl 37 %		Titrate to pH 8,8
	SDS	0,4 % (w/v)	4g
	H_2O		Ad 1 l
4 x upper Tris buffer	1 M Tris-HCl pH 6,8	0,5 M	500 ml
	SDS	0,4 % (w/v)	4 g
	H_2O		Ad 1 l
10 x SDS electro-	Glycin	2 M	334 g
phoresis buffer	Tris	250 mM	30,3 g
	SDS	1 %	10 g
	H_2O		Ad 1 l
6 x Lämmli buffer	1 M Tris-HCl pH 6,8	350 mM	3,5 ml
	SDS	10 % (w/v)	1 g
	β-Mercaptoethanol	5 % (v/v)	500 µl
	Bromphenolblau	0,2 % (w/v)	20 mg
	Glycerol	50 % (v/v)	5 ml
	H_2O		Ad 10 ml
20 % APS	Ammoniumperoxo-	20 % (w/v)	2 g
	sulfat		Ad 10 ml
	H_2O		

Table 12: Recipes for SDS gel electrophoresis buffers and solutions

3.2.2.2 SDS polyacrylamide gel electrophoresis

To separate the proteins by their molecular weight, SDS polyacrylamide gel electrophoresis was performed. Polyacrylamidconcentrations of 6,5 % - 10 % were used for separating gels, 4 % for stacking gels. Gels were either cast in Novex® cassettes or Novex® midi cassettes with a thickness of 1,0 mm using 10 or 20 well combs. Separating gels were cast 1,5 cm below the top cover with a layer of isopropanol. After the separating gel was polymerized, the isopropanol

layer was removed and the stacking gel was casted on top. The combs were inserted immediately. Table 13 shows the recipes for either 5 cassettes or 3 midi cassettes.

Gel		**Separating**		**Stacking**
	6,5 %	**8 %**	**9 %**	**4 %**
Components				
Acryl- Bisacrylamide (30 % / 0,8 %)	6,93 ml	8,53 ml	9,6 ml	2,2 ml
H_2O	15,85 ml	14,25 ml	13,18 ml	10,02 ml
4 x lower Tris buffer	9,00 ml	9,00 ml	9,00 ml	-/-
4 x upper Tris buffer	-/-	-/-	-/-	4,13 ml
20 % APS	180 µl	180 µl	180 µl	83 µl
TEMED	36 µl	36 µl	36 µl	17 µl

Table 13: Recipes for SDS separation and stacking gels

The chamber was filled with 1x SDS Running buffer. Before the samples were added the wells were washed with the ambient buffer. The samples were added with 1 x Lämmli according to the volume of 20 µl. 4 µl BlueEasy Prestained Protein Marker (Nippon Genetics®) was used for protein standard (Figure 6). The run was performed at 160V, 400mA for ca. 50-60 min depending on the gel compositions.

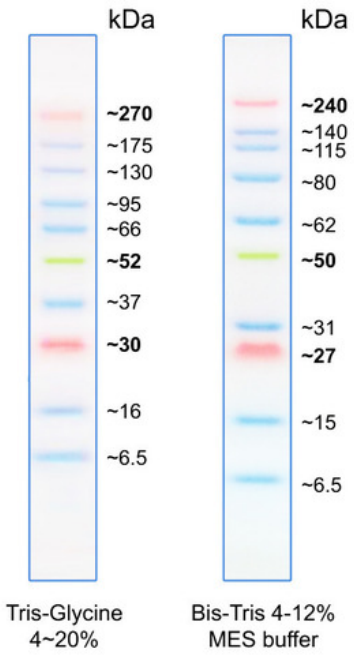

Figure 6: BlueEasy Prestained Protein Marker

3.2.2.3 Western blot

Buffer	Component	Concentration	Amount
Western blot transfer buffer	Tris	25 mM	3 g
	Glycine	192 mM	14,4 g
	SDS	0,02 %	0,2 g
	Methanol	20 %	200 ml
	H_2O		ad 1 l
Western blot blocking buffer	PBS	10 x	100 ml
	Skim Milk powder	5 %	50 g
	Tween 20	0,02 %	2 ml
	H_2O		ad 1l
Western blot washing buffer	PBS	10 x	100 ml
	Tween 20	0,02%	1 ml
	H_2O		ad 1l

Table 14: Recipes for western blot buffers and solutions

After SDS-PAGE, the proteins were transferred on a PVDF membrane by semidry blotting method. The method was original described by Towbin (Towbin, Staehelin, and Gordon 1979). Therefore the PDVF membrane (Merck Millipore®) was incubated for 1 minute in methanol and washed in western blot transfer buffer. The SDS-gels were preincubated for 10 minutes in western blot transfer buffer. The blotting system was assembled as shown in Table *15*. The transfer was performed with BIO-RAD semi dry electro-blot system at 24 V and 400 mA for 80 minutes.

Cathode
3 x Whatman paper
SDS gel
PVDF membrane
3 x Whatman paper
Anode

Table 15: Scheme of western blot assembly

After blotting, the PVDF membrane was blocked over night at 4° C in western blot blocking buffer. There was no washing step performed after blocking. Primary antibodies were diluted 1:1000 and 1:2000 in western blot blocking buffer. The membranes were incubated for 1 h on

a shaker at RT. Then the membranes were washed 3 times for 5 minutes in western blot washing buffer on a shaker. Secondary antibodies were diluted 1:5000 in western blot blocking buffer and given on the membranes for 1 h. Afterwards, the membranes were washed 3 times for 5 minutes in western blot washing buffer on a shaker. For detecting the blotted proteins, the membranes were incubated either in SuperSignal™ West Dura Extended Duration Substrate (Thermo Scientific™) or Westar Supernova™ (Cyanagen®) depending on the expected intensity. Images were taken with FujiFilm LAS-3000 image reader (Fujifilm Holdings Corporation®).

After detection the membranes were treated with western blot blocking buffer, containing 0,02 % sodium acid , overnight to wash off the peroxidase on the secondary antibody. On the next day the membranes were transferred into western blot washing buffer and as necessary after antibody staining reblotted.

Every western blot was followed by coomassie staining (3.2.2.4) of the gel to ensure quantitative transfer of the protein to the membrane.

3.2.2.4 Coomassie staining of SDS gels

After the blotting procedure, the SDS gels were stained in a custom coomassie solution for 15 minutes. Then the gels were destained in hot water using deionized water followed by 30 minutes on a shaker. This step was repeated several times with exchanging the water in between. The destained gels were scanned using Perfection V700 Photo scanner (Seiko Epson Corporation®) and dried with Unigeldryer 3545D (Uniequip®). The gel staining was for means of documentation.

Solution	Component	Concentration	Amount
Custom Coomassie solution	100 % methanol p.A.	50 %	500 ml
	100 % Acetic acid	10 %	100 ml
	Coomassie Brilliant Blue R-250	0,25 % (w/v)	2,5 g
	H_2O		Ad 1l

Table 16: Recipe for Coomassie stain solution

3.2.2.5 Co-immunoprecipitation of CHD3/4 and PU.1 in HEK293 cells

Co-IP experiments were performed with 4,25 - 5 mg WCE in Buffer A in a total volume of 800 µl. For GFP-Trap_A IP (GFP pulldown) with ethidium bromide (EtBr), 10 µg/µl EtBr was added to Buffer A and B in the preclearing as well as in IP step. For Myc-Trap Agarose as well as for GFP-Trap_A without EtBr, buffers shown in
Table 17 were used.

Name	Component	Concentration	Amount
Buffer A	Ex 0 + glycerol	150 mM	16,58 ml
	Ex 1000 + glycerol		3 ml
	Protease Inhibitors	1:50	400 µl
	DTT	1 mM	20 µl
Buffer B	Ex 0 + glycerol	150 mM	274,5 µl
	Ex 1000 + glycerol		75 µl
	Protease Inhibitors	1:50	10 µl
	DTT	1 mM	0,5 µl
	BSA	400 ng/µl	20
	Gelatin	2 %	100
Washing Buffer	Ex 0 + glycerol	500 mM	23,95 ml
	Ex 1000 + glycerol		2,5 ml
	Protease Inhibitors	1:50	100 µl
	DTT	1 mM	5 µl

Table 17: Recipes for IP buffers

According to the manufacture, both trap beads should not be used in solutions higher than 0,2 % detergent. The IP reactions were performed with detergent concentrations of 0,16 - 0,29 %, without detecting any difference in the outcome. Preclearing agarose beads bab-20 and IP trap beads were prepared in a 50 % slurry and initially washed 3 times in 200 µl Buffer A. The lysates were precleared with 50 µl bab-20 agarose bead (Chromotec®) 50 % slurry in buffer A for 1 h at 4° C on a spinning wheel. Both, GFP-Trap_A and Myc-Trap beads were preincubated for 1 h at 4° C in buffer B, also on a spinning wheel. After that, the supernatant was discarded. After preclearing, the supernatant (approx. 750 µl) was transferred after centrifugation (max. 2700g, 1° C, for 1 min) onto the preincubated trap beads (800 µl in total). After 4 h of incubation

the supernatants were collected by centrifugation (max. 2700g, 1° C, for 1 min) and the beads were washed one time in buffer A, one time in washing buffer, followed by two times in buffer A for 5 min at 4° C on a spinning wheel. Between these washing steps, the beads were centrifugated (max. 2700g, 1° C, for 1 min) and the supernatant was discarded. Ultimately, buffer A was removed quantitatively and the beads were resuspended in 60 µl 2 x Laemmli. Also, bab-20 agarose preclearing beads were resuspended in 60 µl 2 x Laemmli. Then both preclearing and trap beads were boiled for 5 minutes at 100° C. After centrifugation (max. 2700g, 1° C, for 1 min) the Laemmli, containing the immunoprecipitated proteins, was collected. The two resulting fractions are further named as preclearing and beads fraction.
All used fractions, preclearing, beads, input and supernatants were shock frozen in liquid nitrogen and frozen on - 80° C. Depending on the estimated amount of immunoprecipitated protein, 1,6 - 33 % of the IP reaction and 50 - 70 µg of Input and Supernatant were used for western blot.

4 Results

4.1 Basic characterization of stable cell lines

To prove the protein interaction between CHD3/CHD4 and PU.1 via co-immunoprecipitation *in vivo*, HEK-293 cells, co-expressing both proteins upon doxycycline induction were chosen as a model organism. Therefore, stable HEK-cell lines were generated by Dr. Helen Hoffmeister and Elisabeth Silberhorn expressing dox-inducible PU.1 tagged with C-Myc-6x-His and either CHD3 or CHD4 coupled with C-terminal GFP-epitope or GFP alone. The cell lines are described and termed according to 3.1.9.

This basic characterization was performed to verify that the inducible expression is reliable and homogenous within the cell population. As a first step, immunocytochemistry (ICC) was performed to determine protein expression levels and to reveal the spatial localization of the tagged proteins in the cells. This was necessary to make sure that no mosaic clones different transfection and expression levels were cultivated. To verify that the tags are bound to their respective proteins, antibody tests were performed. Also, to determine the proteins of interest with the correct size and for validation of suitable antibodies regarding the specificity for further use.

4.1.1 Immunocytochemistry of cell lines

ICC experiments were performed with the three inducible cell lines CHD3-GFP, CHD4-GFP and GFP (see 3.2.1.4). For each cell type the induced and non-induced state was analyzed. The induction time was 24 h and the cells were grown on coverslips. After fixation, cells were permeabilized and stained with an for c-myc-tag with Alexa594 antibody. To visualize nuclear DNA, the cells were also stained with DAPI. Images were recorded in suitable channels for DAPI, GFP, and Alexa594 detection (3.2.1.4).

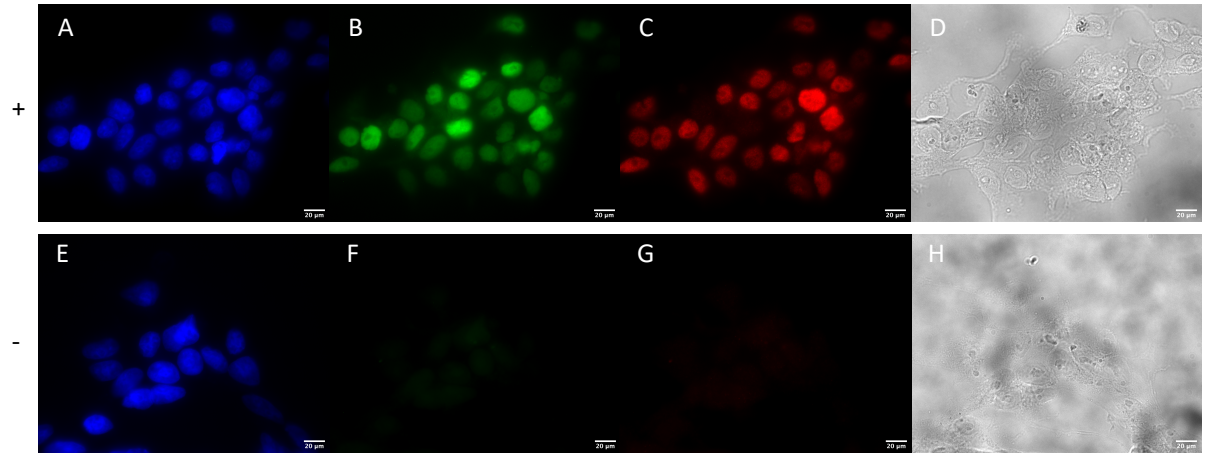

Figure 7: Fluorescence microscopy of induced and non-induced cells expressing CHD3-GFP and PU.1-C-Myc-His.

CHD3-GFP cells were grown on cover slips, induced (+) with doxycycline (shown in the upper panel), fixed, stained and mounted. First staining was performed with an anti-C-Myc-antibody and the secondary fluorescent-labelled Alexa594-antibody. Afterwards, staining with DAPI was performed. Images were recorded for DAPI (A), for GFP fluorescence (B), for red fluorescence (C) and additional brightfield (D). As a control, non-induced (-) HEK293T cells were proceeded accordingly (lower panel, E-H). Measuring bar = 20 µm.

The ICC experiment of CHD3-GFP cells illustrated in Figure *7* show the inducible expression of CHD3-GFP and PU.1-C-Myc-6xHis. In the DAPI channel, induced (A) and non-induced (E), nuclei of regular shape are apparent. In the GFP channel, green fluorescent nuclei, representing GFP-tagged CHD3, can be identified in the induced (B) and being absent in the non-induced cells (F). In the red fluorescence channel (detecting for Alexa594), the expression of PU.1 tagged to C-Myc-6xHis can be observed, upon induction (C, G). Variation in fluorescent intensity represents differences in protein levels depending on varying permeabilized cells. In conclusion, the induced cells expressed the expected GFP- and Myc-tagged proteins and the non-induced control showed significant lower background signal.

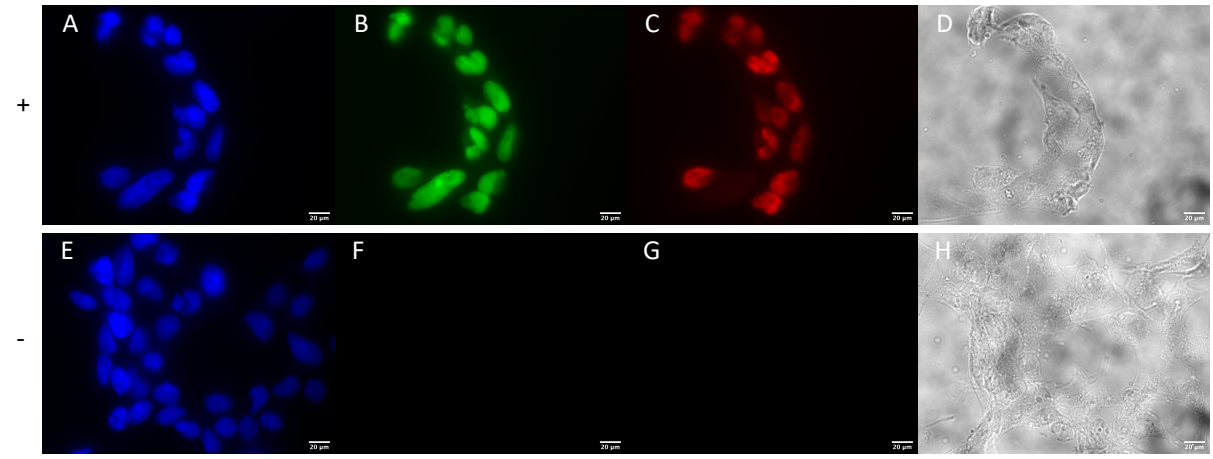

Figure 8: Fluorescence microscopy of induced and non-induced cells expressing CHD4-GFP and PU.1-C-Myc-His.

CHD4-GFP cells were grown on cover slips, induced (+) with doxycycline (shown in the upper panel), fixed and stained and mounted. First staining was performed with an anti-C-Myc-antibody and the secondary fluorescent-labelled Alexa594-antibody. Afterwards, staining with DAPI was performed. Images were recorded for DAPI (A), for GFP fluorescence (B), for red fluorescence (C) and additional brightfield (D). As a control, non-induced (-) HEK293T cells were proceeded accordingly (lower panel, E-H). Measuring bar = 20 µm.

The ICC experiment of CHD4-GFP cells shown in Figure *8* reveal inducible expression of CHD4-GFP and PU.1-cMyc-His. DAPI channel (A, E) and brightfield (D, H) visualize nuclei and cells of proper viability and shape. GFP channel (B, F) and red fluorescence channel (C, G) show induction-dependent expression levels observed in the CHD4-GFP cell line, respectively PU.1-C-Myc-6x-His, comparable with CHD3-GFP. Thus, the induced expression of both proteins could be observed in the CHD4-GFP cell line.

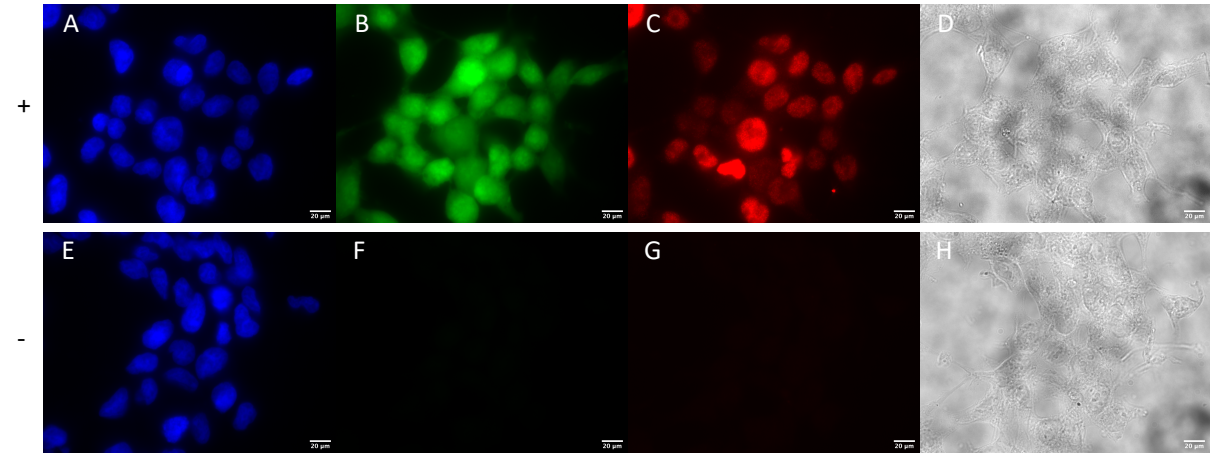

Figure 9: Fluorescence microscopy of induced and non-induced cells expressing GFP and PU.1-C-Myc-His.

GFP cells were grown on cover slips, induced (+) with doxycycline (shown in the upper panel), fixed and stained and mounted. First staining was performed with an anti-C-Myc-antibody and the secondary fluorescent-labelled Alexa594-antibody. Afterwards, staining with DAPI was performed. Images were recorded for DAPI (A), for GFP fluorescence (B), for red fluorescence (C) and additional brightfield (D). As a control, non-induced (-) HEK293T cells were proceeded accordingly (lower panel, E-H). Measuring bar = 20 µm.

The ICC experiment of the control cell line with inducible GFP and PU.1 is shown in Figure *9* and confirm inducible expression of GFP and PU.1-C-Myc-His. As described above, DAPI

channel (A, E) and brightfield (D, H) visualize nuclei and cells of proper viability and shape. GFP channel (B, F) and red fluorescence channel (C, G) show induction-dependent expression of GFP and of PU.1-C-Myc-6x-His. In contrast to CHD3/4-GFP cell lines, GFP is not only located in the nucleus, but also visible in the cytoplasm. This is expected, due to the missing nuclear localization signal of GFP alone, leading to distribution in the whole cell. The induction-dependent expression of GFP and tagged PU.1 could also be confirmed in this cell line.

In summary, all three cell line express inducible and reliable GFP and C-Myc-tag and therefore the CHD proteins or PU.1, which is proven in the following chapter.

4.1.2 Antibody tests

In preparation for the CoIP experiments, western blot analysis were performed to complete the basic characterization protein expression on the one hand and to identify suitable antibodies with regard to their specificity for subsequent experiments on the other hand. In addition, these experiments should reveal whether the proteins are detectable at the correct size in clear dependency of cell induction and no degradation is occurring.
Therefore, induced and non-induced cells of CHD3-GFP, CHD4-GFP and GFP were analyzed in western blot experiments (3.2.2.3) with different antibodies against either CHD3, CHD4, PU.1 or the coupled tags (3.1.9). The cells were induced for 24 h, whole cell extracts (WCE) were prepared (3.2.1.5) and loaded on SDS gels (3.2.2.2).

PU.1 detection

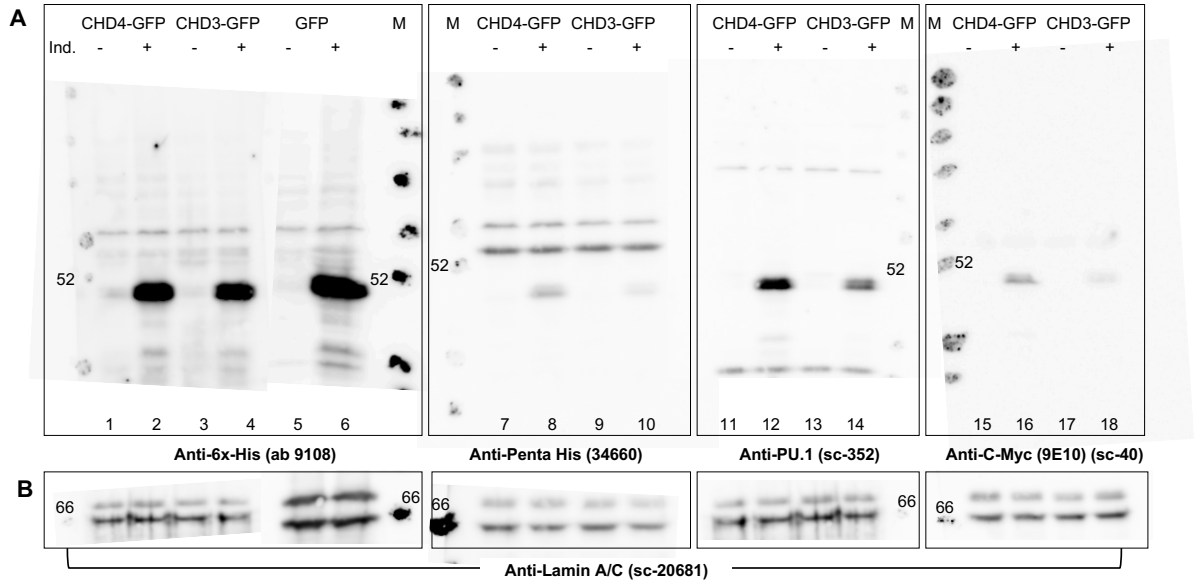

Figure 10: Western blots for antibody test and basic characterization of PU.1 expressing cell lines

Induced (+) and non-induced (-) CHD4-GFP, CHD3-GFP and GFP cells were lysed, protein concentration was determined and 50 µg total protein amount were separated on a 8 % SDS gel and blotted on a PVDF membrane. (A) PU.1-signals were detected with antibodies targeting 6xHis (lane 1-6), 5xHis (lane 7-10), PU.1 (lane 11-14) and C-Myc (lane 15-18) and developed with the SuperSignal West Dura Extende Duration Substrate. (B) As a loading control, membranes were re-blotted with anti-Lamin A/C antibodies and developed accordingly. A protein marker (M) was loaded for size determination and molecular weight levels of interest (kDa) next to the dots are indicated.

Figure 10 shows the western blot to analyze PU.1 expression in induced and non-induced CHD3-GFP and CHD4-GFP cells and GFP cells (A). In the first box, detection with Anti-6x-His was analyzed (lane 1-6). In the induced (+) samples of all three cell lines a clear signal can be observed at the expected molecular weight of below the 52 kDa marker spot (lane 2, 4 6). This signal represents PU.1, which has a molecular weight of 34,7 kDa, and is known to run at a higher size because of post-translational modification. The non-induced (-) samples (lane 1, 3, 5) do not show any clear signal at this height, confirming the PU.1 expression to be induction-dependent. Beside the expected signal, the antibody shows a relatively high background signal in other regions of the blot, representing e.g. unspecific antibody signals.

The second tested antibody, Anti-Penta-His, also targeting the His-tag of PU.1, is shown in the second box (lanes 7-10). In WCE of induced CHD4-GFP cells (lane 8) a weak signal is visible slightly below 52 kDa, while the signal in induced CHD3-GFP (lane 10) is hardly detectable. Since the high expression of PU.1 within these cell lines was already proven (lane 2, 4), this effect is caused by the lacking quality of this antibody.

A third antibody targeting PU.1 directly, Anti-PU.1, was analyzed in lanes 11-14. Using this antibody, induced CHD4-GFP (lane 12) and CHD3-GFP (lane 14) show signals at the correct

height, while the non-induced cells (lane 11, 13) do not. CHD4-GFP exhibit a PU.1 signal of higher intensity compared to CHD3-GFP, indicating differences in expression levels. The background signal of this antibody is relatively low with only a few bands appearing at low molecular weight.
A further antibody, Anti-C-Myc (9E10) targeting the C-Myc-tag, shown in lanes 15-18, revealed a weak signal in general. The induced samples (lanes 16 and 18) do show the expected band below the 52 kDa marker, again with varying intensity between the cell lines, but relatively weak signals. The non-induced samples (lane 15, 17) do not show any signal.
This western blot (A) shows independent of the used antibody that all three cell lines express PU.1-C-Myc-6x-His adequately when induced compared to the not-induced cells, where PU.1 can hardly be detected. In a reblot with Anti-Lamin A/C, shown in B, the loading of equal amounts of protein was confirmed. All lanes show comparable signals at height of 66 kDa and 70 kDa, representing equal amounts of Lamin A and C in all samples.

To determine the optimal antibodies and conditions for PU.1, four antibodies targeting different epitopes were compared. The intensity of the expected PU.1 signal is very weak for the Anti-Penta His and Anti-C-Myc antibodies, making them unacceptable for further experiments. Anti-6x-His and Anti-PU.1 in contrast, exhibit clear signals of high intensity for PU.1. To allude to background signal, the Anti-6xHis shows relatively high background signal in the regions of interest (40-60 kDa), being unsuitable for our purposes, which will require reblots and detection of proteins in this size range on the same membrane. With Anti-PU.1, the background signals of anti-PU.1 below 30 kDa would not affect further IP analysis of reblots. Because of this, finally anti-PU.1 was chosen for all downstream experiments.

CHD3/CHD4/GFP detection

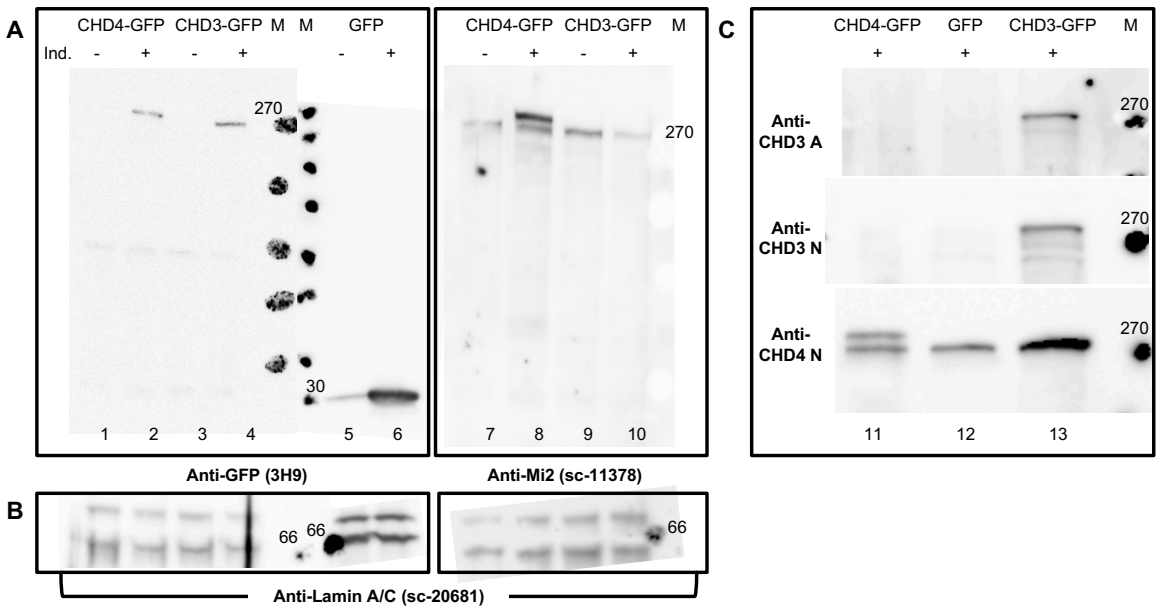

Figure 11: Western blots for antibody test and basic characterization of GFP and CHD expressing cell lines

Induced (+) and non-induced (-) CHD4-GFP, CHD3-GFP and GFP cells were lysed, protein concentration was determined and 50 µg total protein amount were loaded on a 6 - 8 % SDS gel and blotted on a PVDF membrane. (A) CHD-signals were detected with antibodies targeting GFP (lane 1-4) and Mi2 (lane 7-10), only GFP was detected (lane 5-6), and developed with suitable chemiluminescent substrates. (B) As a loading control, membranes were re-blotted with anti-Lamin A/C antibodies and developed accordingly. (C) Induced (+) cell lysates with 70 µg protein concentration were analyzed and CHD3- or CHD4-signals (lane 11-13) were detected with specific antibodies indicated in the figure. A protein marker (M) was loaded for size determination and molecular weight levels of interest (kDa) next to the dots are indicated.

Shown in Figure 11, the same cell clones were tested for CHD3/4 and GFP detection via western blot analysis (3.2.2.3). The first box (A) represents the detection of GFP epitope (anti-GFP) in induced and not induced cell lines CHD3-GFP, CHD4-GFP and GFP (lane 1-6).
All proteins were detected at their expected size. The dox-induced (+) samples display a clear signal with the expected molecular weight of approximately 290 kDa for CHD4 (lane 2, green asterisks) and 275 kDa for CHD3 (lane 4, red asterisks) or a strong signal with 30 kDa for GFP (lane 6). This higher detected sizes (physiological: CHD3: 255 kDa, CHD4: 247 kDa, GFP: 27 kDa) can be traced to post-translation modification. The non-induced (-) samples (lane 1, 3) do not show a signal at this height, confirming the CHD expression to be dox-induction-dependent. In the non-induced sample of GFP (lane 5), a slight but negligible band is visible in the same height, likely caused by spillover. Accordingly, a clear GFP expression increases in signal occurs after induction.

The second tested antibody, Anti-Mi2, targets a common CHD3/4 epitope (lane 7-10) directly. Therefore, endogenous and exogenous CHD3 and CHD4 are detected, which is visible in lane 8. In this lane, the lower band represents the endogenous CHD4, while the upper band

represents the dox-induced exogenous CHD4-GFP fusion (lane 8), which the non-induced lane 7 does not have. As described above, the exogenous larger size can be traced the GFP-tag. The lower intensity in induced CHD3-GFP (lane 10) compared to non-induced (lane 9) indicates questionable antibody properties or high endogenous CHD3 expression in non-induced cells.

In a reblot with Anti-Lamin A/C, shown in B, the loading of equal amounts of protein can be ensured. All lanes show comparable signals at height of 66 kDa and 70 kDa, representing similar amounts of Lamin A and C in all samples.

In addition, further antibodies detecting CHD3 or CHD4 were tested (C). These tests were performed to screen for more sensitive and specific CHD antibodies in induced cells (lane 11-13) and therefore, non-induced cells were neglected. The upper row shows Anti-CHD3_A detecting CHD3 with its expected molecular weight only in the CHD3-GFP cells (lane 13). No notable background signal was ascertainable in the relevant region. Lane 11 and 12 having only endogenous CHD3 show no CHD3 or background signal at all. In the middle row, another Anti-CHD3_N antibody was tested, showing the same results as Anti-CHD3A with additional weak bands below CHD3 indicating degradation products or differently processed CHD3. In the lower row, Anti-CHD4_N was tested, also showing a consistent signal at the expected size for CHD3 through all cell lines, representing endogenous CHD proteins. CHD4-GFP cells (lane 11) show in addition a band at 290 kDa, identified as exogenous CHD4. As the investigated cell lines were chosen from an IP input shown in 4.2.1, no loading controls were performed.

This western blot (A) shows that the three cell lines express respectively CHD3-GFP, CHD4-GFP or GFP only when induced compared to the not-induced cells. For CHD3-GFP, detection of endogenous and induced expressed CHD3 highly depends on the used antibody.

For optimal CHD detection the Anti-GFP antibody was chosen for all following experiments. This antibody showed clear signals for exogenous CHD3 and CHD4 with no background signals, no signal for non-induced cells and because of economic reasons.

It was possible to show an induction dependent protein expression and a suitable detection through all used cell lines, CHD3-GFP, CHD4-GFP and GFP. The ICC experiments showed that induction results in an increase of expression of the respective proteins with no or less background signal. In the subsequently antibody tests, the induced cells were detectable and sufficiently distinguishable from the non-induced cells with the selected antibodies for the following experiments: Anti-GFP, Anti-PU.1. Therefore, all requirements for the co-immunoprecipitation experiments are fulfilled.

4.2 Co-immunoprecipitation of CHD3/4 and PU.1 in HEK293 cells

The aim of this study was to investigate the interaction of the remodeling enzyme CHD3/4 and the transcription factor PU.1 in context of living cells. In order to prove this potential interaction, co-immunoprecipitation experiments with cell lines dox-inducibly expressing CHD3/4-GFP and PU.1-C-Myc-6xHis were performed. The interaction was investigated by the immunoprecipitation of CHD3/4-GFP and PU.1 separately and detection of the putative interaction partner.
In the first approach, pulldown with the GFP antibody was performed, precipitating the associated CHD protein and potential interaction partners. The IP fractions were analyzed by western blot for presence of PU.1 and in addition for proteins of the NuRD remodeling complex, which has been evidenced to interact with CHD3/4 (Hoffmeister et al. 2017). The second CoIP was performed by pulling down PU.1 via its C-Myc-tag and the detection of CHD proteins and NuRD subunits within the IP fractions.

4.2.1 Identification of CHD3/4 interactors after GFP pulldown

The CHD3-GFP, CHD4-GFP and GFP cell lines were induced with dox for 24 h and whole cell extracts were prepared (3.2.1.5). After determining the protein concentration (3.2.2.1), 5 mg were used to perform one co-immunoprecipitation experiment using GFP-Trap_A beads (0). Subsequently, the four obtained fractions (Preclearing, Beads, Input and Supernatant) were loaded on SDS gels (3.2.2.2) and analyzed via western blot (3.2.2.3), using antibodies against GFP, PU.1 and known members of the NuRD complex: MTA2, RbAp46 and HDAC1. The GFP expressing cell line served as a negative control.

The same experiment was repeated with a 2nd batch of WCEs obtained from an independent dox induction.

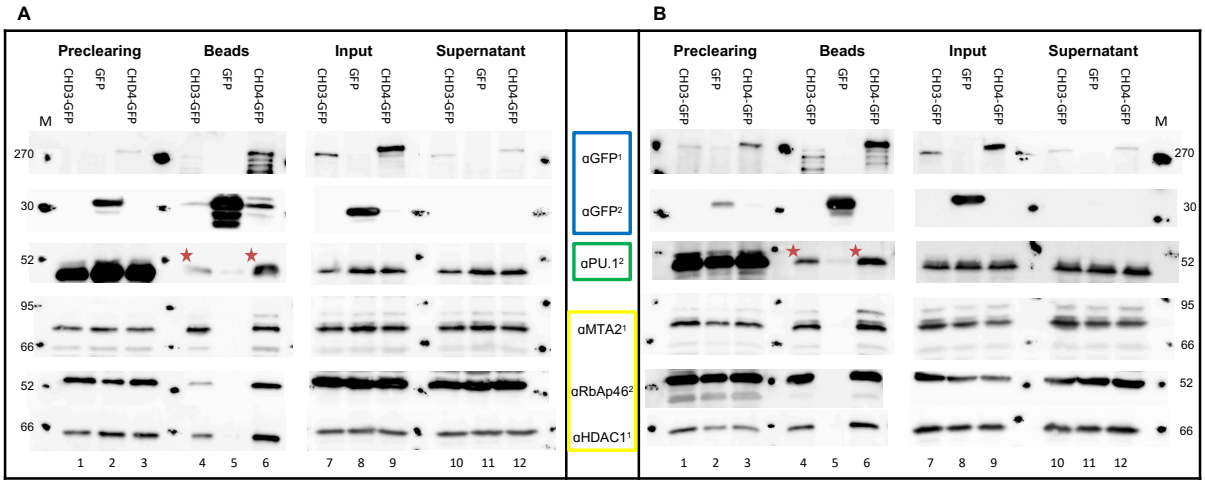

Figure 12: Western blot analysis of co-Immunoprecipitation with GFP pulldown

5 mg WCE of induced CHD3-GFP (lane 1, 4, 7, 10), GFP (lane 2, 5, 8, 11) and CHD4-GFP (lane 3, 6, 9, 12) cell lines were used for CoIP experiments and the fraction Preclearing, Beads, Input and Supernatant were loaded on 6,5 % ([1]) and 9 % ([2]) SDS gel and blotted on a PVDF membrane. Protein signals of CHD and GFP (bait proteins, blue box), PU.1 (prey protein, green box) and NuRD subunits (MTA2, RbAp46, HDAC1, yellow box) were detected with antibodies shown in the figure and developed with suitable chemiluminescent substrates. A and B represent replicates of the experiment with different protein amounts loaded: (A) 8 % of Preclearing and Beads, 70 µg of Input and Supernatant on a 6,5 % SDS gel; 17 % of the Preclearing and Beads, 70 µg of Input and Supernatant on a 9 % SDS gel. (B) 17 % of Preclearing and Beads (1,7 % for GFP), 70 µg of Input and Supernatant on a 6,5 % SDS gel; 25 % of Preclearing and Beads, 70 µg of Input and Supernatant on a 9 % SDS gel. A protein marker (M) was loaded for size determination and molecular weight levels of interest (kDa) are indicated. Detection of PU.1 in GFP pulldown samples are indicated with red asterisks.

Figure *12* shows two biological replicates (A and B) of the co-immunoprecipitation with GFP out of CHD3-GFP, CHD4-GFP and GFP. The following description is applicable for both replicates.

The first two rows show the detection of the bait protein GFP or CHD3/4-GFP using the anti-GFP antibody (blue box). In the CHD3-GFP and CHD4-GFP samples, signals in the size of CHD with 270/290 kDa could be observed, while the GFP sample shows GFP bands at 30 kDa size. As described before, the exogenous larger size can be traced to the larger size of the GFP-tagged CHD proteins (4.1.2).

The fractions differ in signal intensity: The input fractions clearly show the presence of the proteins CHD3-GFP (lane 7), GFP (lane 8) or CHD4-GFP (lane 9) respectively. In the preclearing fraction (lane 1-3), which was used to minimize unspecific binding in general, no or minimal signal for CHD3/4-GFP is visible, and a moderate signal for GFP in the second row can be seen. This excludes widely unspecific binding of CHD3/4-GFP. The beads fractions show a minimal CHD3-GFP signal in A and a strong signal in B (respectively lane 4), a very strong GFP signal (lane 5) and a clear CHD4-GFP signal (lane 6), confirming binding of GFP and GFP-tagged proteins to the GFP pulldown beads. The supernatant fractions represent the non-bound proteins after the bead incubation and show a significant depletion in (CHD3/4-)

GFP signal intensity (lane 10-12) suggesting efficient binding of the tagged proteins to the beads.
In order to test for CHD3/4-PU.1 interaction, the fractions were analyzed for the presents of PU.1 below 50 kDa with the Anti-PU.1 antibody (third panel, green box). The input fraction (lane 7-9) all show comparable signal for PU.1, confirming the similar expression within the three cell lines. Strong signals could be detected in the preclearing fractions (lane 1-3), demonstrating strong unspecific binding to agarose beads and serves as a washing step. With the GFP-pulldown in the Beads fractions, we observe a clear PU.1 signal in the cell lines expressing CHD3-GFP (lane 4) and CHD4-GFP (lane 6) - marked with red asterisks - and hardly any signal for the control cell line (lane 5). **This data supports a direct or indirect interaction between CHD3/4 and PU.1 in vivo.** The supernatant fractions exhibit clear signals for PU.1 in all cell lines (lane 10-12) showing the abundance of PU.1 in the lysates.

Furthermore, a set of NuRD subunits (yellow box) known to interact with CHD3/4 were detected using Anti-MTA2, Anti-RbAp46 and Anti-HDAC1 antibodies (lower part). In all input fraction (lane 7-9), in all preclearing fraction (lane 1-3) and in all supernatant fraction (10-12) consistent signal for the enzymes MTA2 at 75 kDa, RbAp46 above 50 kDa and HDAC1 at 62 kDa can be observed. With the GFP bait in the Beads fractions, all three NuRD subunits were pulled down in CHD3-GFP (lane 4) and CHD4-GFP (lane 6), but not in the GFP control (lane 5). These results suggest that PU.1 interacts with CHDs in the context of NuRD.

To summarize, the described CoIP (Figure *12*) was successful in terms of pulling down GFP and the attached CHD proteins (bait). With that, we could show the co-immunoprecipitation of PU.1 (prey), and thus, the specific interaction with CHD3/4 *in vivo*. Additionally, the known existence of CHD3/4 in the context of the NuRD complex could be proven by detecting three of its known core subunits. Comparing CHD3-GFP (lane 4) and CHD4-GFP (lane 6) cell lines, clear differences in expression levels of all proteins have to be annotated, which can be traced upon the exogenous CHD proteins and the endogenous NuRD subunits.
The observed interaction between PU.1 and CHD3/4 is suggested to be a direct protein-protein interaction (Fuchs, Andreas 2013; Tedesco, Nadja 2017). To exclude a DNA-mediated interaction, the Co-IP experiments were performed in the presence of ethidium bromide.

4.2.2 The interaction between PU.1 and NuRD is not mediated by DNA

The analysis performed in 4.2.1 to identify CHD3/4 interactors by CoIP experiments were repeated by supplementing the GFP-Trap A reaction with 200 ng ethidium bromide, to exclude the interaction to be DNA-mediated (0).

Therefore, the cell lines CHD3-GFP, CHD4-GFP and GFP were dox-induced for 24 h and whole cell extracts were prepared (3.2.1.5). Cell lysates containing 5 mg protein were used to perform one co-immunoprecipitation experiments using GFP-Trap_A (0). The four obtained fractions (Preclearing, Beads, Input and Supernatant) were loaded on a SDS gel (3.2.2.2) and analyzed via western blot (3.2.2.3). The analysis repetitively consists of bait protein detection, PU.1 detection and NuRD subunit MTA2, RbAp46 and HDAC1 detection by parallelly cutting the western blot membrane. The GFP expressing cell line served again as a negative control. The identical experiment was repeated with a 2nd batch of WCEs from the same dox-induction.

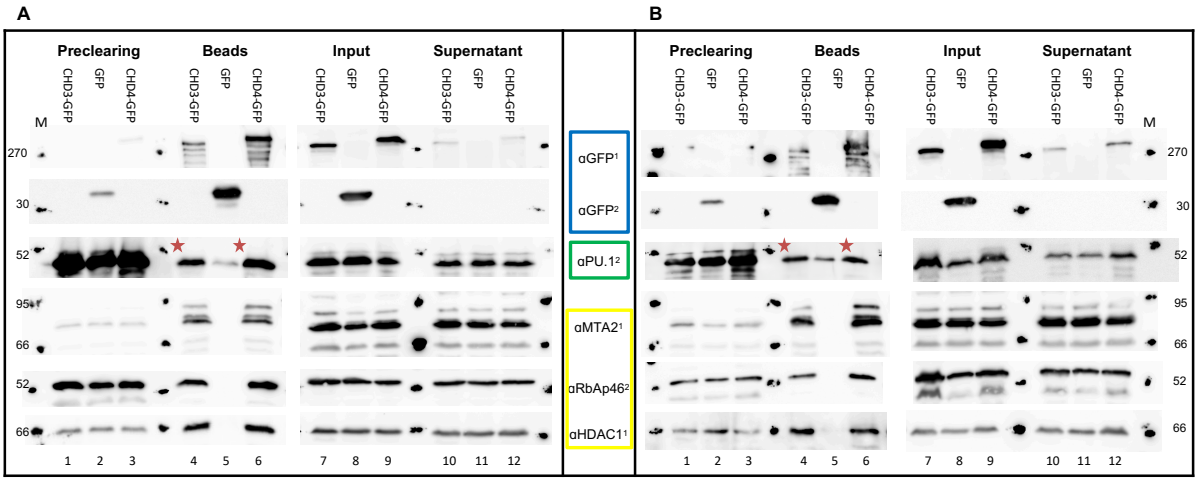

Figure 13: Western blot analysis of Co-Immunoprecipitation with GFP pulldown in presence of ethidium bromide

5 mg WCE of induced CHD3-GFP (lane 1, 4, 7, 10), GFP (lane 2, 5, 8, 11) and CHD4-GFP (lane 3, 6, 9, 12) cell lines were used for CoIP experiments with ethidium bromide and the fraction Preclearing, Beads, Input and Supernatant were loaded on 6,5 % ([1]) and 9 % ([2]) SDS gel and blotted on a PVDF membrane. Protein signals of CHD and GFP (bait proteins, blue box), PU.1 (prey protein, green box) and NuRD subunits (MTA2, RbAp46, HDAC1, yellow box) were detected with antibodies shown in the figure and developed with suitable chemiluminescent substrates. A and B represent replicates of the experiment with following protein amounts loaded:17 % of Preclearing and Beads, 70 µg of Input and Supernatant on a 6,5 % SDS gel; 25 % of the Preclearing and Beads (1,7 % for GFP), 70 µg of Input and Supernatant on a 9 % SDS gel. A protein marker (M) was loaded for size determination and molecular weight levels of interest (kDa) are indicated. Detection of PU.1 in GFP pulldown samples are indicated with red asterisks.

Figure *13* shows two biological replicates (A and B) of the co-immunoprecipitation with GFP pulldown in presence of ethidium bromide of CHD3-GFP, CHD4-GFP and GFP, further characterizing the interaction of PU.1 and CHD3/4. The following description is applicable for both replicates (A and B):

The first two panels (*Figure 13*) contain the detection of the bait protein GFP or CHD3/4-GFP (yellow box) in the four IP fractions (see above) using the anti-GFP antibody. It shows the successful pulldown of those proteins in the CoIP, as described in 4.2.1. Ethidium bromide obviously does not affect the pulldown. Therefore, the interaction between PU.1 and CHD4/4 is not mediated by DNA.

In order to characterize the observed CHD3/4-PU.1 interaction, the fractions were analyzed for PU.1 with the anti-PU.1 antibody (third panel, prey protein). Again, the fractions in the EtBr-CoIP show the same results as the previous IP in 4.2.1. With the GFP-pulldown we obtain a clear PU.1 signal in the cell lines expressing CHD3 (lane 4) and CHD4 (lane 6) - marked with red asterisks - and hardly any signal for the control cell line (lane 5). This repetitively confirms the direct interaction between CHD3/4 and PU.1 and excludes the interaction to be DNA-mediated, but rather based on protein-protein interaction.

The detection of the NuRD subunits, using anti-MTA2, anti-RbAp46 and anti-HDAC1 antibodies (lower part) widely confirms the results observed in 4.2.1. An observed deviation is the reduced signal in the preclearing fraction (lane 1-3) for MTA2 determination. This effect could potentially be caused by ethidium bromide or other experimental parameters. But again, all three NuRD components were shown to interact with CHD3/4, **independent of DNA**.

To conclude, the presence of ethidium bromide in the otherwise identically performed CoIP (Figure *13* compared to Figure *12*) did not exhibit any major differences. **Which means, the observed interactions of CHD3/4 and the addressed proteins *in vivo* are shown to be protein-protein-based and not DNA-mediated.**

4.2.3 Identification of PU.1 interactors after C-Myc-pulldown

The interaction between CHD3/4 and PU.1 in context of living cells was sucessfully shown by pulling down GFP and thus CHD3/4. To analyse this interaction from the other way round, PU.1 was co-immunoprecipitated via its C-Myc tag and analysed for CHD3/4 interaction in the context of NuRD.
The previously used cell lines CHD3-GFP, CHD4-GFP and GFP were dox-induced for 24 h and WCEs were prepared (3.2.1.5). Cell extracts with 4,25 mg total protein amount were used to perform a co-immunoprecipitation experiment using Myc-Trap agarose beads (0). The

obtained fractions (Preclearing, Beads, Input and Supernatant) were loaded on a SDS gel (3.2.2.2). The western blot analysis includes the detection of the bait protein (PU.1, blue box), the expected interactors CHD3 and CHD4 (prey proteins, green box) and their interaction partners in form of NuRD core subunits such as MTA2, RbAp46, HDAC1 (yellow box). The GFP cell line serves as a negative control. The identical experiment was repeated with a 2nd batch of WCEs from a different dox induction.

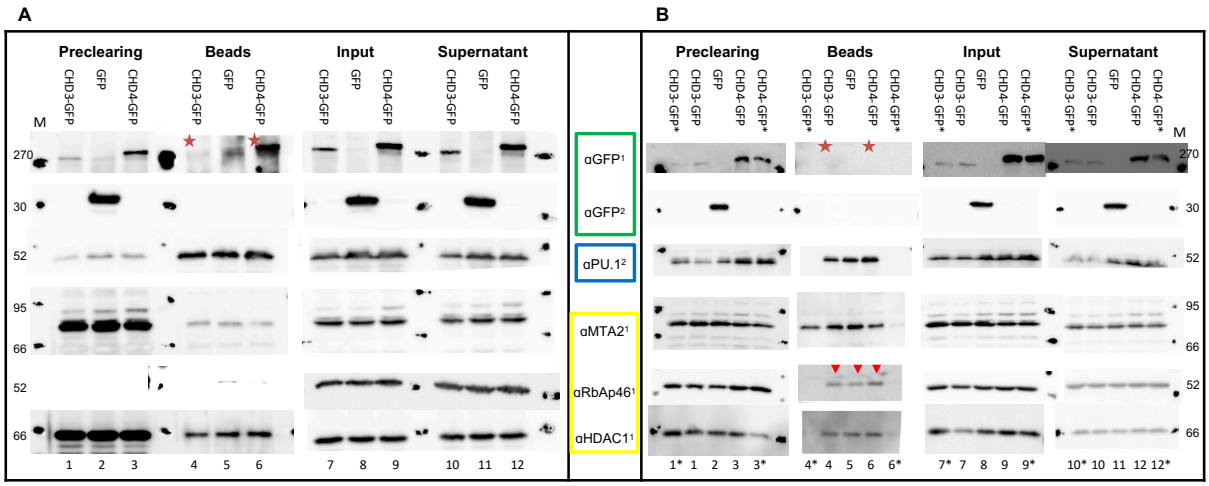

Figure 14: Western blot analysis of Co-Immunoprecipitation with C-Myc pulldown

5 mg WCE of induced CHD3-GFP (lane 1, 4, 7, 10), GFP (lane 2, 5, 8, 11) and CHD4-GFP (lane 3, 6, 9, 12) cell lines were used for CoIP experiments and the fraction Preclearing, Beads, Input and Supernatant were loaded on 6,5 % and 9 % SDS gel and blotted on a PVDF membrane. Protein signals of CHD, GFP, PU.1 and NuRD subunits (MTA2, RbAp46, HDAC1) were detected with antibodies shown in the figure and developed with suitable chemiluminescent substrates. A and B represent replicates of the experiment with different protein amounts and additional protein fractions loaded: (A) 33 % of Preclearing and Beads, 70 µg of Input and Supernatant on a 6,5 % SDS gel; 12,5 % of the Preclearing and Beads, 70 µg of Input and Supernatant on a 9 % SDS gel. (B) 33 % of Preclearing and Beads, 50 µg of Input and Supernatant on a 6,5 % SDS gel; 12,5 % of the Preclearing and Beads, 50 µg of Input and Supernatant on a 9 % SDS gel. Additional fractions of CHD3-GFP (lane 1*, 4*, 7*, 10*) and CHD4-GFP (lane 3*, 6*, 9*, 12*) incubated a second time with preclearing beads instead of trap beads were analyzed (marked with *). A protein marker was loaded for size determination and molecular weight levels of interest (kDa) are indicated. Detection of CHD in GFP pulldown samples are indicated with red asterisks. Red triangles are shown to highlight the weak signal of RbAp46 (B lane 4-6).

Figure 14 shows two of six replicates (A and B) of the co-immunoprecipitation with cMyc pulldown out of CHD3-GFP, CHD4-GFP and GFP.

In A, the third panel contains the detection of the bait protein PU.1-cMyc-6xHis using the anti-PU.1 antibody. In all cells lines, CHD3-GFP, CHD4-GFP, GFP, signals in the size of PU.1 below 50 kDa could be observed. The fractions differ in signal intensity: The input fractions clearly show the presence of the PU.1 protein (lane 7-9). In the preclearing fraction (lane 1-3) no or minimal signal for PU.1 is visible widely revealing low levels of unspecific binding. The beads fractions show a clear and consistent PU.1 signal (lane 4-6), confirming the binding of PU.1 to the Myc-Trap beads. The supernatant fractions represent the non-bound proteins after

the bead incubation and do not show a significant decrease in signal intensity (lane 10-12) emphasizing PU.1 abundance.

In order to confirm CHD3/4-PU.1 interaction, the fractions were analyzed for a signal of CHD3/4 and GFP only with the anti-GFP antibody (second panel, prey protein, green box). The input fractions show signals for CHD3–GFP (lane 7), GFP only (lane 8) and CHD4-GFP (lane 9) in the size of 270/30/290 kDa, confirming the expression of the proteins in the three cell lines. As described before, the exogenous higher detected sizes can be traced to post-translational modification (4.1.2). In the Beads fractions, we observe a weak signal in the cell line expressing CHD3 (lane 4) and a clear signal for CHD4 (lane 6) - marked with red asterisks - and hardly any signal for the control cell line (lane 5). This would support the hypothesized interaction between CHD3/4 and PU.1. However, the supernatant fractions exhibit clear signals for (CHD3/4)-GFP in all cell lines (lane 10-12) comparable to the input, indicating non-efficient binding to PU.1, bound to the beads.

The analyzed NuRD core subunits known to interact with CHD3/4 were detected using anti-MTA2, anti-RbAp46 and anti-HDAC1 antibodies (yellow box). In all input fraction (lane 7-9), in all preclearing fraction (lane 1-3) and in all supernatant fraction (10-12) consistent signal for the enzymes MTA2 at 75 kDa, RbAP46 above 50 kDa and HDAC1 at 62 kDa can be observed, confirming the abundance of these enzymes in the cells. With the cMyc bait in the Beads fractions, all three NuRD subunits were pulled down in all cell line, CHD3-GFP (lane 4) and CHD4-GFP (lane 6), as well as in the GFP control cell line (lane 5). Since the NuRD core subunits could be detected in all three samples, we could not prove the interaction with PU.1 to be CHD3/4 dependent.

In B, two additional flanking samples for each fraction (marked with *) were analyzed, containing the CHD3/4-GFP cells incubated with agarose prebeads instead of Myc-Trap beads. This serves as an additional control evaluated the specificity of the preclearing beads.

The third panel contains the detection of the bait protein PU.1-cMyc-6xHis using the anti-PU.1 antibody (blue box). In CHD3-GFP, CHD4-GFP, GFP samples signals in the size of PU.1 below 50 kDa could be observed of similar signal intensity in all fractions (lane 1-12). An exception represent the differently treated *samples, which do not show a PU.1 signal in the Beads fraction (lane 4*, 6*). This is caused by the preclearing beads, that do not include Myc-Trap and thus, not pulling down PU.1 unspecifically.

The CHD3/4 detection (first panel, green box) in the replicate B could not confirm the results of replicate A in terms of co-immunoprecipitating CHD proteins with PU.1, being representative for the lacking reproducibility in four more replicates.
The analysis of the NuRD subunits showed in principle consistent results with A. Small deviations occurred sporadically, e.g. detection problem of RbAp46 (B, lane 4-6), marked with red triangles.

In summary, the results of the cMyc-IP could show a successful pulldown of the bait protein and also the NuRD core subunits, which could be replicated. The detection of the CHD proteins could be shown (Figure 14, A, red asterisks), but was not replicatable (Figure 14, B, red asterisks). This does not disprove the interaction between PU.1 and CHD proteins, and thus with the NuRD core subunits. Due to this results, no Co-IP pulling down C-Myc in presence of EtBr was performed. Putative reasons for inconsistent results in the two IP approaches are discussed in 5.2.

5 Discussion

5.1 Comparison of both CoIPs and their conclusions for further investigations

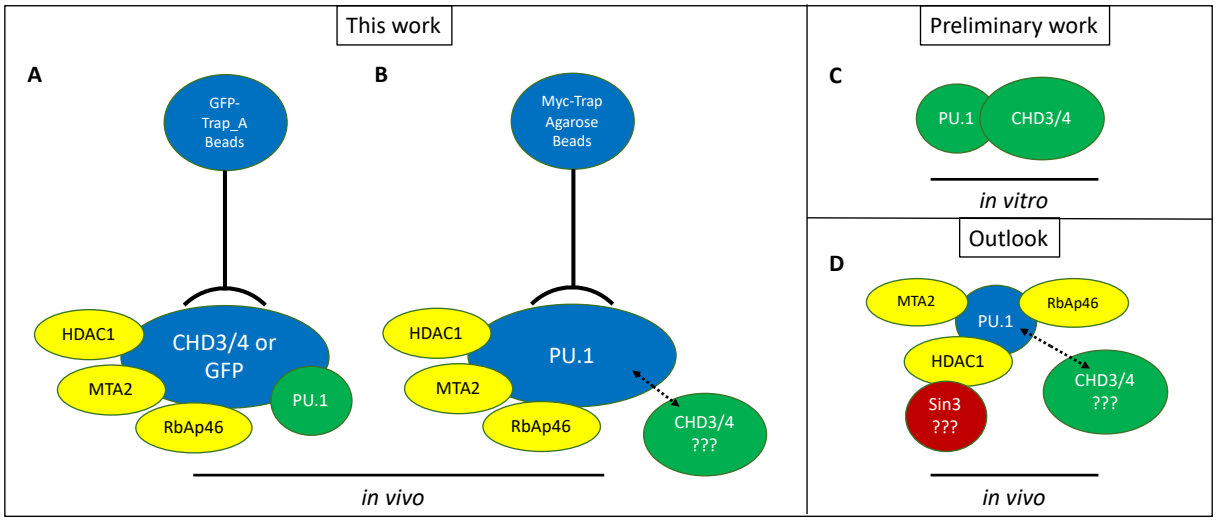

Figure 15: Schematic compilation investigated interactions

A: CoIP with GFP pulldown. It was possible to detect the bait protein CHD3/4, which confirms the technical aspect of the experiment. Also, the prey protein PU.1 and subsequently the known NuRD core subunits (yellow ovals) were sufficiently detectable. **B:** CoIP with cMyc pulldown. The detection of the bait protein PU.1 was successful, confirming the immunoprecipitation. The further analysis of the prey proteins CHD3/4 exposed detection problems in replicability (dotted arrow). The known NuRD core subunits (yellow ovals) were sufficiently detectable. **C:** Schematic compilation of preliminary results. **D:** Schematic compilation of the investigated interaction with further suggestion (red balloon). Detection of CHD3/4 exposed sensitivity issues (dotted arrow).

Figure 15 shows a schematic overview to preliminary (C) and current result (A, B). Andreas Fuchs and Nadja Tedesco (both this lab) have recently shown that hCHD3 and hCHD4 do directly interact with hPU.1 *in vitro* (C). Here, we used stabily transfected, dox-inducible cells co-expressing CHD3-GFP/PU.1, CHD4-GFP/PU.1 and GFP/PU.1 (3.1.9). The cell lines were prepared by co-immunoprecipitation for the interaction of CHD3/4 and PU.1 in the context of the NuRD remodeling complex. NuRD is composed of its core subunits MTA2, RbAp46 and HDAC1 (A and B; 4.2). The GFP pulldown CoIP (A) clearly showed the protein-protein interaction of CHD3/4 (blue balloon) with PU.1 (green balloon) in context of the NuRD complex (yellow balloons). Furthermore the interaction was shown to be independent of DNA, suggesting a functional interaction *in vivo*. This confirms the described *in vitro* interaction (Andreas Fuchs, Nadja Tedesco, data not shown). The detailed character and network of the protein interaction distinct in this complex needs to be further investigated (6). With the findings within the cMyc CoIP (B), it was possible to detect the bait protein PU.1 (blue balloon) and subsequently the known NuRD core subunits (yellow balloons). The verified, DNA

independent interaction (0) remains unilateral, as it exposed a detection issue in replicability in points of CHD3/4 detection in the PU.1 pulldown (4.2.3, Figure 14, red asterisks). This would not disprove our results (D), but has to be discussed in points of technical issues and assumable interactions with other complexes (red balloon).

5.2 Evaluation of the interactions

5.2.1 Method optimization

As the results in 0 confirm a DNA independent interaction of CHD3/4 and PU.1, CHD3/4 were hardly detectable in the CoIP vice versa (4.2.3). However, both IP reactions were performed under the same conditions, errors to the method should be considered and evaluated. According to the manufacturer, the used Trap Beads (3.1.2) should not be used in solutions containing more than 0,2 % detergent. As Andreas Fuchs described functional IP reactions below 0,28 % IGEPAL CA-630 (Fuchs, Andreas 2013), we accomplished to keep the detergent below the critical limit of 0,2 % by an average of 0,18 %. Also, unspecific binding could already been excluded by blocking the beads with BSA and gelatin for 1 h before the incubation (0) as well as secondly incubating the IP input with preclearing beads (Figure 14, lanes marked with *). The analysis of the preclearing beads did not show any remarkable unspecific binding to the beads. In principle, the unequivocal detection of the bait protein in both IPs implies the pulldown method to be functional. Furthermore, as we assume in the following, limited amounts of CHD3/4 are responsible for the non-replicability. Therefore, we advise to re-investigate the PU.1-pulldown CoIP ultimately by mass spectrometry. This would maximize the sensitivity to detect the hypothesized interacting partner.

5.2.2 Putative factors influencing the protein interaction

The considered influences on the method did not raise any clarifying issues yet. Therefore we suggest, the non-replicability to be substantiated in the interactions itself. The character of the artificial expression system and the differences to the unaltered natural environment should also be considered.

Artificial model in HEK system/HEK cells as a model system

As preliminary work of Nadja Tedesco with THP cells expressing endogenous PU.1 upon differentiation to macrophages was not sufficient in points of cultivation, differentiation and expression levels (Tedesco, Nadja 2017), we decided to generate stabile transfected HEK293 cells (3.1.9). Due to an easier transfection and cultivation as well as a sufficient amount of protein required for the upcoming IP and ChIP experiments (6), this model system was chosen. It has to be noted, that this is an artificial system, as PU.1 is not physiologically expressed in these cells. The question remains, does this model meet the unaltered requirements or are the described detection problems (4.2.3) due to this model system. Cells physiologically expressing PU.1 and also CHD proteins like hematopoietic cell lineages or even mesenchymal stem cells MSCs could enlighten this issue (Gu et al. 2014).
However it has to be noted, the investigated proteins are tagged (3.1.9) and expression levels are highly artificial under control of a strong promoter. Therefore, artificial overexpression is a fundamental precondition to this examined interaction. As the basic characterization showed a sufficient and correct protein localization (4.1) and our IP experiments (4.2) reproducibly verified published interaction partners for CHD3/4 and PU.1 (Ahringer 2000; Hoffmeister et al. 2017), the depict artificial struggles should be neglected.

Detection of exogenous versus endogenous CHD

The WCE used in the CoIP experiments (3.2.1.5) contained exogenous as well as endogenous proteins. The overexpressed exogenous proteins are further tagged, which makes it possible to perfunctory differentiate between endogenous and exogenous interaction partners.
Analyzing the GFP pulldown CoIP (4.2.1, 0), only GFP tagged CHD proteins are immunoprecipitated. As it was possible to co-immunoprecipitate the prey protein PU.1 via an anti-PU.1 antibody, endo- as well as exogenous PU.1 could be detected (4.1.2). Anyway, we expect the HEK cells not to express endogenous PU.1. The detected NuRD core subunit are exclusively endogenous. The other way round, pulling down PU.1 by its cMyc-tag contains exclusively exogenous PU.1 and interacting CHD proteins, both exo- and endogenous. As it was possible to detect the core subunits of the NuRD complex (4.2.3), it showed difficulties in detecting the prey NuRD motor protein CHD3/4. The CHD proteins were detected via an anti-GFP antibody, which thus only detects the exogenous variant.

The question to address, is it a matter of frequency, if an endo- or exogenous CHD is incorporated in the detected NuRD complex? As CHD3/4-GFP has undergone an enrichment by the GFP pulldown, it may have been easier to detect the protein by its tag (4.2.3). This issue could be evaluated by using an antibody having its epitope in the CHD aa sequence. Not mentioned in the literature before, having problems with detection of incorporated tagged proteins, it suggests to be a matter of sensitivity. As already investigated in 4.1.2, our available direct CHD antibodies failed to fulfill the requirements. This opens the possibility to further investigate this issue by using a suitable antibody.

Binding of PU.1 to beads affects interaction

The lacking of CHD detection could be conceivable reasoned in the binding of PU.1 via its cMyc-tag to the beads. So far, it cannot be precluded to affect the successive interaction with distinct partners. Supposing the binding blocks the epitope for PU.1-CHD3/4 interaction, it would be an option to replace the cMyc beads with either Ni^{2+}-beads for the c-terminal His-tag or protein A- or G beads coupled antibodies having their epitope directly in the PU.1 aa sequence. However, the latter is questionable, as the assumption is: blocked epitopes. If the binding of PU.1 to the cMyc beads does not directly block any epitope relevant for interaction, different protein folding could be another reason or due to the binding, the stability of the interaction between PU.1 and CHD3/4 is affected. This could be supported by the suggestion that PU.1 binds via its ETS domain to the PHD zinc finger region of CHD3/4. The distance between the cMyc region and the ETS-binding domain is short with min. 5 aa (Takahashi 2011; P. Zhang et al. 2000). In comparison, within the GFP pulldown CoIP the distance between the N-terminal PHD domain to the GFP-tag located at the C-terminus is more than 1500 aa plus its own tag length and thus, not affecting the interaction.

5.3 Putative PU.1 interaction within a different complex

As it was difficult to detect CHD3/4 by pulling down PU.1 by its cMyc tag, there is reason to suggest, that PU.1 is incorporated in different complexes. Analyzing the detected NuRD core subunits, it is conspicuous that the Sin3 complex shares the most of its core subunits with NuRD, inherent HDAC1/2 and RbAp 46/48 (Ahringer 2000; Y. Zhang et al. 1999)

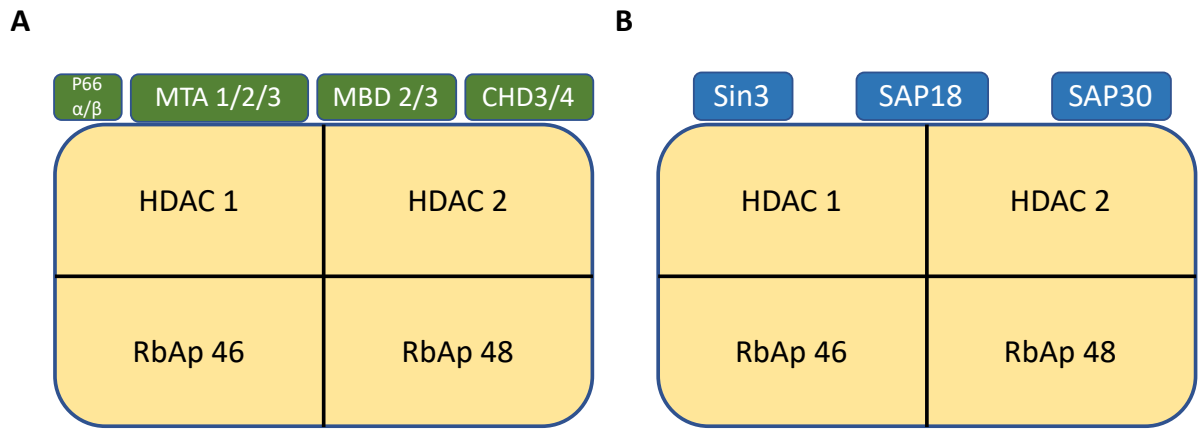

Figure 16: Comparison of the NuRD and Sin3 complex

The yellow boxes (A and B) show the shared core subunits of the NuRD and Sin3 complex. **A:** Shows the known core subunits of the NuRD complex. The NuRD specific subunits are highlighted in green boxes. **B:** Shows the known core subunits of the Sin3 complex, The Sin3 specific subunits are highlighted in blue boxes (modified from Ahringer 2000).

Figure 16 shows a comparison of the known NuRD and Sin3 core subunits. This assumption could be supported by detecting HDAC1 and RbAp 46 in the CoIPs (4.2.3). Therefore, it could be suggested, that PU.1 rather interacts within the Sin3 complex, explaining the detection issues of CHD3/4 in the CoIP. As there was no Sin3 antibody available, no other Sin3 subunit was analyzed, and therefore no justification can be made at this point. This suggestion could be investigated by detecting Sin3 exclusive subunits such as sin3a, SAP18 (**s**in3a **a**ssociated **p**rotein) or SAP30.

Architecture of the interaction

Since we could not detect CHD in the PU.1 pulldown but several other NuRD subunits, the question arises which proteins and accordingly which domains are mediating the PU.1-NuRD interaction. Taking a closer look to the other detected protein, the detection of MTA2 which remains to be NuRD specific, proves the PU.1-NuRD interaction (Fujita et al. 2004; H. Zhang, Stephens, and Kumar 2006). Therefore, the suggestion should be analyzed focusing on PU.1

and its direct interacting partners. As Hoffmeister et al. showed the direct interaction between PU.1 and CHD3/4 (Hoffmeister et al. 2017), it was already described, that PU.1 is also able to interact with HDAC1 (Johnstone 2002).

This leads to the assumption that not exclusively CHD3/4 mediates the binding to PU.1 and NuRD, but another subunit does. It is already described, PU.1 is able to interact with Sin3A, HDAC1, NuRD and other proteins like Dnmt1, Prmt5 and CoRest (Gu et al. 2014, Kelly and Cowley 2013). But the exact architecture of the interaction between PU.1 and CHD3/4 is not described yet. So far it is assumed that the ETS domain of PU.1 interacts with CHD via its zinc-finger domain (P. Zhang et al. 2000). This fact allows the hypothetical possibility, that PU.1 interacts via its ETS-domain also with other zinc-finger domain. Beside CHD, the mentioned proteins within NuRD, except HDAC1, also possess zinc-finger domains. These could potentially mediate the PU.1 interaction. Thus, the detection of the NuRD subunits in the CHD negative control could be explained.

6 Conclusion

In summary, the performed CoIP experiments showed an protein-protein interaction between CHD3/4 and PU.1 (4.2.1), which revealed to be DNA independent (0). This interaction could be proven unilateral, with an assumed sensitivity problem preventing bilaterality (4.2.3).
To further examine this issue, the CoIP pulling down PU.1 via its cMyc-tag should be investigated by mass spectrometry. An alternative option to prove PU.1-CHD3/4 interaction would be the optimization of the cellular expression system. In this context, a cellular model with physiological conditions should be examined additionally.
Furthermore, a putative interaction between PU.1 and NuRD subunits should be investigated in *in vitro* and *in vivo* experiments to clarify a possible interaction network. This could be achieved by CoIPs of purified recombinant proteins analogue to the preliminary work of Nadja Tedesco and Andreas Fuchs (Fuchs, Andreas 2013; Tedesco, Nadja 2017)
Also, it should be considered that PU.1 is interacting with other complexes, since the protein was proven to be involved in numerous transcription associated processes (Gu et al. 2014; Kelly and Cowley 2013). Another interesting question represents the identification of DNA loci and binding sites interacting with PU.1. In order to address this question, ChIP experiments with the established PU.1 expressing cell lines should be performed.
An unequivocal verification of the interaction between PU.1 and CHD3/4 leaving following questions open: What is the relevance of the interaction of CHD3/4 and PU.1 in the cellular context? Is there a variation across specific cell types? Which impact does this have cellular processes such as transcription. How is the interaction regulated?.

7 Literature

Ahringer, J. 2000. “NuRD and SIN3 Histone Deacetylase Complexes in Development.” *Trends in genetics: TIG* 16(8): 351–56.

Akashi, K., D. Traver, T. Miyamoto, and I. L. Weissman. 2000. “A Clonogenic Common Myeloid Progenitor That Gives Rise to All Myeloid Lineages.” *Nature* 404(6774): 193–97.

Anderson, M. K., G. Hernandez-Hoyos, R. A. Diamond, and E. V. Rothenberg. 1999. “Precise Developmental Regulation of Ets Family Transcription Factors during Specification and Commitment to the T Cell Lineage.” *Development (Cambridge, England)* 126(14): 3131–48.

Anderson, Michele K. et al. 2002. “Constitutive Expression of PU.1 in Fetal Hematopoietic Progenitors Blocks T Cell Development at the pro-T Cell Stage.” *Immunity* 16(2): 285–96.

Ball, L. J. et al. 1997. “Structure of the Chromatin Binding (Chromo) Domain from Mouse Modifier Protein 1.” *The EMBO journal* 16(9): 2473–81.

Bannister, Andrew J., and Tony Kouzarides. 2011. “Regulation of Chromatin by Histone Modifications.” *Cell Research* 21(3): 381–95.

Basta, J., and M. Rauchman. 2017. “The Nucleosome Remodeling and Deacetylase Complex in Development and Disease.” In *Translating Epigenetics to the Clinic*, Elsevier, 37–72. https://linkinghub.elsevier.com/retrieve/pii/B9780128008027000034 (September 3, 2019).

Becker, Peter B., and Wolfram Hörz. 2002. “ATP-Dependent Nucleosome Remodeling.” *Annual Review of Biochemistry* 71: 247–73.

Behre, G. et al. 1999. “C-Jun Is a JNK-Independent Coactivator of the PU.1 Transcription Factor.” *The Journal of Biological Chemistry* 274(8): 4939–46.

Bradford, M. M. 1976. “A Rapid and Sensitive Method for the Quantitation of Microgram Quantities of Protein Utilizing the Principle of Protein-Dye Binding.” *Analytical Biochemistry* 72: 248–54.

Breiling, Achim, and Frank Lyko. 2015. “Epigenetic Regulatory Functions of DNA Modifications: 5-Methylcytosine and Beyond.” *Epigenetics & Chromatin* 8: 24.

Buratowski, S. 1994. “The Basics of Basal Transcription by RNA Polymerase II.” *Cell* 77(1): 1–3.

Burda, P., P. Laslo, and T. Stopka. 2010. “The Role of PU.1 and GATA-1 Transcription Factors during Normal and Leukemogenic Hematopoiesis.” *Leukemia* 24(7): 1249–57.

Chen, H. et al. 1995. “PU.1 (Spi-1) Autoregulates Its Expression in Myeloid Cells.” *Oncogene* 11(8): 1549–60.

Clapier, Cedric R., and Bradley R. Cairns. 2009. “The Biology of Chromatin Remodeling

Complexes." *Annual Review of Biochemistry* 78: 273–304.

Cook, Wendy D. et al. 2004. "PU.1 Is a Suppressor of Myeloid Leukemia, Inactivated in Mice by Gene Deletion and Mutation of Its DNA Binding Domain." *Blood* 104(12): 3437–44.

Davey, Curt A. et al. 2002. "Solvent Mediated Interactions in the Structure of the Nucleosome Core Particle at 1.9 a Resolution." *Journal of Molecular Biology* 319(5): 1097–1113.

Denslow, S. A., and P. A. Wade. 2007. "The Human Mi-2/NuRD Complex and Gene Regulation." *Oncogene* 26(37): 5433–38.

Donaldson, L. W., J. M. Petersen, B. J. Graves, and L. P. McIntosh. 1996. "Solution Structure of the ETS Domain from Murine Ets-1: A Winged Helix-Turn-Helix DNA Binding Motif." *The EMBO journal* 15(1): 125–34.

Eeckhoute, Jéröme, Raphaël Métivier, and Gilles Salbert. 2009. "Defining Specificity of Transcription Factor Regulatory Activities." *Journal of Cell Science* 122(Pt 22): 4027–34.

Eisenbeis, C. F., H. Singh, and U. Storb. 1995. "Pip, a Novel IRF Family Member, Is a Lymphoid-Specific, PU.1-Dependent Transcriptional Activator." *Genes & Development* 9(11): 1377–87.

Eltsov, Mikhail et al. 2008. "Analysis of Cryo-Electron Microscopy Images Does Not Support the Existence of 30-Nm Chromatin Fibers in Mitotic Chromosomes in Situ." *Proceedings of the National Academy of Sciences of the United States of America* 105(50): 19732–37.

Felsenfeld, Gary, and Mark Groudine. 2003. "Controlling the Double Helix." *Nature* 421(6921): 448–53.

Flanagan, John F. et al. 2005. "Double Chromodomains Cooperate to Recognize the Methylated Histone H3 Tail." *Nature* 438(7071): 1181–85.

Flaus, Andrew, David M. A. Martin, Geoffrey J. Barton, and Tom Owen-Hughes. 2006. "Identification of Multiple Distinct Snf2 Subfamilies with Conserved Structural Motifs." *Nucleic Acids Research* 34(10): 2887–2905.

Friedman, A. D. 2007. "Transcriptional Control of Granulocyte and Monocyte Development." *Oncogene* 26(47): 6816–28.

Fuchs, Andreas. 2013. "Characterisation of CHD3 and CHD4 Chromatin Remodelling Enzymes." University of Regensburg.

Fujita, Naoyuki et al. 2003. "MTA3, a Mi-2/NuRD Complex Subunit, Regulates an Invasive Growth Pathway in Breast Cancer." *Cell* 113(2): 207–19.

———. 2004. "MTA3 and the Mi-2/NuRD Complex Regulate Cell Fate during B Lymphocyte Differentiation." *Cell* 119(1): 75–86.

Fulton, Debra L. et al. 2009. "TFCat: The Curated Catalog of Mouse and Human Transcription

Factors.” *Genome Biology* 10(3): R29.

Fussner, Eden, Reagan W. Ching, and David P. Bazett-Jones. 2011. “Living without 30nm Chromatin Fibers.” *Trends in Biochemical Sciences* 36(1): 1–6.

Gertz, Jason et al. 2012. “Genistein and Bisphenol A Exposure Cause Estrogen Receptor 1 to Bind Thousands of Sites in a Cell Type-Specific Manner.” *Genome Research* 22(11): 2153–62.

Goebl, M. K. 1990. “The PU.1 Transcription Factor Is the Product of the Putative Oncogene Spi-1.” *Cell* 61(7): 1165–66.

Greenberg, Maxim V. C., and Deborah Bourc’his. 2019. “The Diverse Roles of DNA Methylation in Mammalian Development and Disease.” *Nature Reviews Molecular Cell Biology* 20(10): 590–607.

Gu, Xiaorong et al. 2014. “Runx1 Regulation of Pu.1 Corepressor/Coactivator Exchange Identifies Specific Molecular Targets for Leukemia Differentiation Therapy.” *The Journal of Biological Chemistry* 289(21): 14881–95.

Gururaj, Anupama E. et al. 2006. “MTA1, a Transcriptional Activator of Breast Cancer Amplified Sequence 3.” *Proceedings of the National Academy of Sciences of the United States of America* 103(17): 6670–75.

Hagemeier, C., A. J. Bannister, A. Cook, and T. Kouzarides. 1993. “The Activation Domain of Transcription Factor PU.1 Binds the Retinoblastoma (RB) Protein and the Transcription Factor TFIID in Vitro: RB Shows Sequence Similarity to TFIID and TFIIB.” *Proceedings of the National Academy of Sciences of the United States of America* 90(4): 1580–84.

Hashimoto, Hideharu et al. 2012. “Recognition and Potential Mechanisms for Replication and Erasure of Cytosine Hydroxymethylation.” *Nucleic Acids Research* 40(11): 4841–49.

Hausner, W., and M. Thomm. 2001. “Events during Initiation of Archaeal Transcription: Open Complex Formation and DNA-Protein Interactions.” *Journal of Bacteriology* 183(10): 3025–31.

Hendrich, B., and A. Bird. 1998. “Identification and Characterization of a Family of Mammalian Methyl-CpG Binding Proteins.” *Molecular and Cellular Biology* 18(11): 6538–47.

Hoffmeister, Helen et al. 2017. “CHD3 and CHD4 Form Distinct NuRD Complexes with Different yet Overlapping Functionality.” *Nucleic Acids Research* 45(18): 10534–54.

Hollenhorst, Peter C., Lawrence P. McIntosh, and Barbara J. Graves. 2011. “Genomic and Biochemical Insights into the Specificity of ETS Transcription Factors.” *Annual Review of Biochemistry* 80(1): 437–71.

Hong, Wei et al. 2005. “FOG-1 Recruits the NuRD Repressor Complex to Mediate Transcriptional Repression by GATA-1.” *The EMBO journal* 24(13): 2367–78.

Hromas, R. et al. 1993. “Hematopoietic Lineage- and Stage-Restricted Expression of the ETS Oncogene Family Member PU.1.” *Blood* 82(10): 2998–3004.

Johnson, P. F., and S. L. McKnight. 1989. “Eukaryotic Transcriptional Regulatory Proteins.” *Annual Review of Biochemistry* 58: 799–839.

Johnstone, Ricky W. 2002. “Histone-Deacetylase Inhibitors: Novel Drugs for the Treatment of Cancer.” *Nature Reviews Drug Discovery* 1(4): 287–99.

Kelly, Richard D. W., and Shaun M. Cowley. 2013. “The Physiological Roles of Histone Deacetylase (HDAC) 1 and 2: Complex Co-Stars with Multiple Leading Parts.” *Biochemical Society Transactions* 41(3): 741–49.

Klemsz, M. J. et al. 1990. “The Macrophage and B Cell-Specific Transcription Factor PU.1 Is Related to the Ets Oncogene.” *Cell* 61(1): 113–24.

Kruithof, Maarten et al. 2009. “Single-Molecule Force Spectroscopy Reveals a Highly Compliant Helical Folding for the 30-Nm Chromatin Fiber.” *Nature Structural & Molecular Biology* 16(5): 534–40.

Lambert, Samuel A. et al. 2018. “The Human Transcription Factors.” *Cell* 172(4): 650–65.

Längst, Gernot, and Peter B. Becker. 2004. “Nucleosome Remodeling: One Mechanism, Many Phenomena?” *Biochimica et Biophysica Acta (BBA) - Gene Structure and Expression* 1677(1–3): 58–63.

Längst, Gernot, and Laura Manelyte. 2015. “Chromatin Remodelers: From Function to Dysfunction.” *Genes* 6(2): 299–324.

Li, Xiao, and Xiang-Dong Fu. 2019. “Chromatin-Associated RNAs as Facilitators of Functional Genomic Interactions.” *Nature Reviews Genetics* 20(9): 503–19.

Luger, K., and T. J. Richmond. 1998. “DNA Binding within the Nucleosome Core.” *Current Opinion in Structural Biology* 8(1): 33–40.

Mansfield, Robyn E. et al. 2011. “Plant Homeodomain (PHD) Fingers of CHD4 Are Histone H3-Binding Modules with Preference for Unmodified H3K4 and Methylated H3K9.” *The Journal of Biological Chemistry* 286(13): 11779–91.

McKercher, S. R. et al. 1996. “Targeted Disruption of the PU.1 Gene Results in Multiple Hematopoietic Abnormalities.” *The EMBO journal* 15(20): 5647–58.

Miyamoto, Toshihiro et al. 2002. “Myeloid or Lymphoid Promiscuity as a Critical Step in Hematopoietic Lineage Commitment.” *Developmental Cell* 3(1): 137–47.

Moreau-Gachelin, F. 1994. “Spi-1/PU.1: An Oncogene of the Ets Family.” *Biochimica Et Biophysica Acta* 1198(2–3): 149–63.

Moreau-Gachelin, F., A. Tavitian, and P. Tambourin. 1988. “Spi-1 Is a Putative Oncogene in

Virally Induced Murine Erythroleukaemias." *Nature* 331(6153): 277–80.

Murzina, Natalia V. et al. 2008. "Structural Basis for the Recognition of Histone H4 by the Histone-Chaperone RbAp46." *Structure (London, England: 1993)* 16(7): 1077–85.

Musselman, Catherine A. et al. 2009. "Binding of the CHD4 PHD2 Finger to Histone H3 Is Modulated by Covalent Modifications." *The Biochemical Journal* 423(2): 179–87.

———. 2012. "Bivalent Recognition of Nucleosomes by the Tandem PHD Fingers of the CHD4 ATPase Is Required for CHD4-Mediated Repression." *Proceedings of the National Academy of Sciences of the United States of America* 109(3): 787–92.

Nagulapalli, S., J. M. Pongubala, and M. L. Atchison. 1995. "Multiple Proteins Physically Interact with PU.1. Transcriptional Synergy with NF-IL6 Beta (C/EBP Delta, CRP3)." *Journal of Immunology (Baltimore, Md.: 1950)* 155(9): 4330–38.

Nair, Sujit S., Da-Qiang Li, and Rakesh Kumar. 2013. "A Core Chromatin Remodeling Factor Instructs Global Chromatin Signaling through Multivalent Reading of Nucleosome Codes." *Molecular Cell* 49(4): 704–18.

Nelsen, B. et al. 1993. "Regulation of Lymphoid-Specific Immunoglobulin Mu Heavy Chain Gene Enhancer by ETS-Domain Proteins." *Science (New York, N.Y.)* 261(5117): 82–86.

Nerlov, C., E. Querfurth, H. Kulessa, and T. Graf. 2000. "GATA-1 Interacts with the Myeloid PU.1 Transcription Factor and Represses PU.1-Dependent Transcription." *Blood* 95(8): 2543–51.

Pearce, J. J., P. B. Singh, and S. J. Gaunt. 1992. "The Mouse Has a Polycomb-like Chromobox Gene." *Development (Cambridge, England)* 114(4): 921–29.

Pongubala, J. M. et al. 1993. "Effect of PU.1 Phosphorylation on Interaction with NF-EM5 and Transcriptional Activation." *Science (New York, N.Y.)* 259(5101): 1622–25.

Pongubala, J. M., and M. L. Atchison. 1997. "PU.1 Can Participate in an Active Enhancer Complex without Its Transcriptional Activation Domain." *Proceedings of the National Academy of Sciences of the United States of America* 94(1): 127–32.

Pray-Grant, Marilyn G. et al. 2005. "Chd1 Chromodomain Links Histone H3 Methylation with SAGA- and SLIK-Dependent Acetylation." *Nature* 433(7024): 434–38.

Rekhtman, N., F. Radparvar, T. Evans, and A. I. Skoultchi. 1999. "Direct Interaction of Hematopoietic Transcription Factors PU.1 and GATA-1: Functional Antagonism in Erythroid Cells." *Genes & Development* 13(11): 1398–1411.

Robinson, Philip J. J., Louise Fairall, Van A. T. Huynh, and Daniela Rhodes. 2006. "EM Measurements Define the Dimensions of the '30-Nm' Chromatin Fiber: Evidence for a Compact, Interdigitated Structure." *Proceedings of the National Academy of Sciences of the*

United States of America 103(17): 6506–11.

Roche, Andrea E. et al. 2008. "The Zinc Finger and C-Terminal Domains of MTA Proteins Are Required for FOG-2-Mediated Transcriptional Repression via the NuRD Complex." *Journal of Molecular and Cellular Cardiology* 44(2): 352–60.

Saha, Anjanabha, Jacqueline Wittmeyer, and Bradley R. Cairns. 2006. "Chromatin Remodelling: The Industrial Revolution of DNA around Histones." *Nature Reviews. Molecular Cell Biology* 7(6): 437–47.

Scott, E. W., M. C. Simon, J. Anastasi, and H. Singh. 1994. "Requirement of Transcription Factor PU.1 in the Development of Multiple Hematopoietic Lineages." *Science (New York, N.Y.)* 265(5178): 1573–77.

Seelig, H. P. et al. 1995. "The Major Dermatomyositis-Specific Mi-2 Autoantigen Is a Presumed Helicase Involved in Transcriptional Activation." *Arthritis and Rheumatism* 38(10): 1389–99.

Si, Wenzhe et al. 2015. "Dysfunction of the Reciprocal Feedback Loop between GATA3- and ZEB2-Nucleated Repression Programs Contributes to Breast Cancer Metastasis." *Cancer Cell* 27(6): 822–36.

Takahashi, Shinichiro. 2011. "PU.1, a Versatile Transcription Factor and a Suppressor of Myeloid Leukemia." In *Myeloid Leukemia - Basic Mechanisms of Leukemogenesis*, ed. Steffen Koschmieder. InTech. http://www.intechopen.com/books/myeloid-leukemia-basic-mechanisms-of-leukemogenesis/pu-1-a-versatile-transcription-factor-and-a-suppressor-of-myeloid-leukemia (November 17, 2019).

Tedesco, Nadja. 2017. "Functional and Structural Characterization of the Interaction between PU.1 with CHD3 and CHD4." University of Regensburg.

Tong, J. K. et al. 1998. "Chromatin Deacetylation by an ATP-Dependent Nucleosome Remodelling Complex." *Nature* 395(6705): 917–21.

Towbin, H., T. Staehelin, and J. Gordon. 1979. "Electrophoretic Transfer of Proteins from Polyacrylamide Gels to Nitrocellulose Sheets: Procedure and Some Applications." *Proceedings of the National Academy of Sciences of the United States of America* 76(9): 4350–54.

Vaquerizas, Juan M., Sarah K. Kummerfeld, Sarah A. Teichmann, and Nicholas M. Luscombe. 2009. "A Census of Human Transcription Factors: Function, Expression and Evolution." *Nature Reviews. Genetics* 10(4): 252–63.

Wade, P. A., P. L. Jones, D. Vermaak, and A. P. Wolffe. 1998. "A Multiple Subunit Mi-2 Histone Deacetylase from Xenopus Laevis Cofractionates with an Associated Snf2 Superfamily ATPase." *Current biology: CB* 8(14): 843–46.

Watson, Aleksandra A. et al. 2012. “The PHD and Chromo Domains Regulate the ATPase Activity of the Human Chromatin Remodeler CHD4.” *Journal of Molecular Biology* 422(1): 3–17.

Wei, Gong-Hong et al. 2010. “Genome-Wide Analysis of ETS-Family DNA-Binding in Vitro and in Vivo.” *The EMBO journal* 29(13): 2147–60.

Woodage, T. et al. 1997. “Characterization of the CHD Family of Proteins.” *Proceedings of the National Academy of Sciences of the United States of America* 94(21): 11472–77.

Woodcock, Christopher L., and Rajarshi P. Ghosh. 2010. “Chromatin Higher-Order Structure and Dynamics.” *Cold Spring Harbor Perspectives in Biology* 2(5): a000596.

Wreggett, K. A. et al. 1994. “A Mammalian Homologue of Drosophila Heterochromatin Protein 1 (HP1) Is a Component of Constitutive Heterochromatin.” *Cytogenetics and Cell Genetics* 66(2): 99–103.

Xue, Y. et al. 1998. “NURD, a Novel Complex with Both ATP-Dependent Chromatin-Remodeling and Histone Deacetylase Activities.” *Molecular Cell* 2(6): 851–61.

Zhang, Hao, L. Clifton Stephens, and Rakesh Kumar. 2006. “Metastasis Tumor Antigen Family Proteins during Breast Cancer Progression and Metastasis in a Reliable Mouse Model for Human Breast Cancer.” *Clinical Cancer Research: An Official Journal of the American Association for Cancer Research* 12(5): 1479–86.

Zhang, P. et al. 2000. “PU.1 Inhibits GATA-1 Function and Erythroid Differentiation by Blocking GATA-1 DNA Binding.” *Blood* 96(8): 2641–48.

Zhang, Y. et al. 1999. “Analysis of the NuRD Subunits Reveals a Histone Deacetylase Core Complex and a Connection with DNA Methylation.” *Genes & Development* 13(15): 1924–35.

Acknowledgements

An dieser Stelle möchte ich mich bei all denjenigen bedanken, die mich während meiner Doktorarbeit begleitet, unterstützt und gefördert haben.

Mein Dank gilt zunächst Herrn Prof. Dr. Gernot Längst, meinem Doktorvater, für die gute Betreuung der letzten Jahre und die Themenstellung, die mir einen runden Abschluss meines vorangegangenen Studiums der Biochemie ermöglicht hat. Danke für die stetige Unterstützung und den konstruktiven Austausch.

Ich möchte mich ebenfalls bei Prof. Dr. Matthias Mack für das Übernehmen des Zweitgutachtens bedanken.

Ich möchte mich herzlichst bei Frau Dr. Helen Hoffmeister für die engagierte Einarbeitung und die stetige Unterstützung bedanken. Danke für deine Geduld und deinen Einsatz.

Vielen Dank an meine Familie und dabei vor allem Josef Siegel. Lieber Papa, danke, dass du mir diesen Weg ermöglicht hast und immer für mich da bist.

Mein besonderer Dank gilt jedoch Maresa Watzlowik, die mich jeden Tag im Labor und Zuhause unterstützt hat, sowie Nadja Tedesco, dass ich fachlich sowie emotional an ihr Projekt anknüpfen konnte. Danke für all den fachlichen Austausch, eure Unterstützung und eure stets offenen Ohren.